Real-Time Forecasting for the Antarctic: An Evaluation of the Antarctic Mesoscale Prediction System (AMPS)*

DAVID H. BROMWICH AND ANDREW J. MONAGHAN

Polar Meteorology Group, Byrd Polar Research Center, and Atmospheric Sciences Program, Department of Geography, The Ohio State University, Columbus, Ohio

KEVIN W. MANNING AND JORDAN G. POWERS

Mesoscale and Microscale Meteorology Division, National Center for Atmospheric Research, Boulder, Colorado

(Manuscript received 29 January 2004, in final form 19 August 2004)

ABSTRACT

In response to the need for improved weather prediction capabilities in support of the U.S. Antarctic Program's field operations, the Antarctic Mesoscale Prediction System (AMPS) was implemented in October 2000. AMPS employs the Polar MM5, a version of the fifth-generation Pennsylvania State University–NCAR Mesoscale Model optimized for use over ice sheets. The modeling system consists of several domains ranging in horizontal resolution from 90 km covering a large part of the Southern Hemisphere to 3.3 km over the complex terrain surrounding McMurdo, the hub of U.S. operations. The performance of the 30-km AMPS domain versus observations from manned and automatic weather stations is statistically evaluated for a 2-yr period from September 2001 through August 2003. The simulated 12–36-h surface pressure and near-surface temperature at most sites have correlations of $r > 0.95$ and $r > 0.75$, respectively, and small biases. Surface wind speeds reflect the complex topography and generally have correlations between 0.5 and 0.6, and positive biases of 1–2 m s^{-1}. In the free atmosphere, $r > 0.95$ (geopotential height), $r > 0.9$ (temperature), and $r > 0.8$ (wind speed) at most sites. Over the annual cycle, there is little interseasonal variation in skill. Over the length of the forecast, a gradual decrease in skill is observed from hours 0–72. One exception is the surface pressure, which improves slightly in the first few hours, due in part to the model adjusting from surface pressure biases that are caused by the initialization technique over the high, cold terrain.

The impact of the higher-resolution model domains over the McMurdo region is also evaluated. It is shown that the 3.3-km domain is more sensitive to spatial and temporal changes in the winds than the 10-km domain, which represents an overall improvement in forecast skill, especially on the windward side of the island where the Williams Field and Pegasus runways are situated, and in the lee of Ross Island, an important area of mesoscale cyclogenesis (although the correlation coefficients in these regions are still relatively low).

1. Introduction

After the early-season medical evacuation of Dr. Jerri Nielsen from Amundsen-Scott South Pole Station in October 1999 (Nielsen 2001), the U.S. Antarctic Program aimed to improve numerical weather forecasting capabilities to support Antarctic aircraft operations. Soon after, in May 2000, the National Science Foundation sponsored the Antarctic Weather Forecasting Workshop at the Byrd Polar Research Center of The Ohio State University (OSU; Bromwich and Cassano 2001). As a result of that meeting and trial runs established earlier in the year at OSU that showed the feasibility of real-time mesoscale atmospheric modeling for Antarctica, the Antarctic Mesoscale Prediction System (AMPS) was implemented in October 2000. AMPS is an experimental system run at the Mesoscale and Microscale Meteorology (MMM) Division of the National Center for Atmospheric Research (NCAR) and dedicated to real-time numerical weather prediction in Antarctica (Powers et al. 2003; http://www.mmm.ucar.edu/rt/mm5/amps/). AMPS employs the Polar MM5, a version of the fifth-generation Pennsylvania State University–NCAR (PSU–NCAR) Mesoscale Model (MM5; Grell et al. 1995) optimized for the environment of polar ice sheets by the Polar Meteorology Group of

* Byrd Polar Research Center Contribution Number 1301.

Corresponding author address: Andrew J. Monaghan, Polar Meteorology Group, Byrd Polar Research Center, The Ohio State University, 1090 Carmack Road, Columbus, OH 43210.
E-mail: monaghan@polarmet1.mps.ohio-state.edu

the Byrd Polar Research Center (Bromwich et al. 2001; Cassano et al. 2001; http://polarmet.mps.ohio-state.edu). AMPS is a collaborative effort between NCAR's MMM group and OSU. The role of MMM is to run AMPS twice daily, provide a Web interface and model products to the United States and the international forecasting community, and maintain the model code. The role of OSU is to continue development of the model physics and to evaluate the system's performance.

AMPS consists of six domains (Fig. 1): 1) a 90-km grid domain covering a large portion of the Southern Hemisphere; 2) a 30-km grid domain over the Antarctic continent; 3) a 10-km grid domain covering the western Ross Sea; 4) a 3.3-km grid domain covering the immediate Ross Island region (the hub of the U.S. Antarctic Program); 5) a 10-km grid domain encompassing Amundsen-Scott South Pole Station; and 6) a 10-km grid domain enclosing the Antarctic Peninsula (this domain is not evaluated in this text, as it was only implemented in September 2003). A general overview of AMPS is provided by Powers et al. (2003), along with a description of two noteworthy international rescue efforts in which AMPS provided invaluable forecast guidance. Since that publication, the system provided guidance for another South Pole medical evacuation in September 2003. Because of its experimental status, AMPS is very flexible, and changes to the system are not required to go though an extensive review process. This has allowed special windows and products to be implemented on short notice to assist in focused field activities and rescues. One example is a suite of tailored products over the Antarctic Peninsula region in support of the National Science Foundation's Global Ocean Ecosystem Dynamics program.

Bromwich et al. (2003) examined the performance of the AMPS 10-km domain during a combined synoptic/mesoscale event in the western Ross Sea in January 2001. They found that the model reproduced the evolution of upper-level conditions in agreement with observations and resolved near-surface mesoscale features such as topographically induced high/low vortices. They also noted that the accuracy of the forecasts was strongly dependent on the quality of the initial conditions despite the relatively high resolution. Monaghan et al. (2003) compared the performance of AMPS with several other models during the ~1 week period leading up to the late-season rescue of Dr. Ronald Shemenski, a medical doctor seriously ill with pancreatitis, from the South Pole in April 2001. They found that in general, each of the four models examined [AMPS; the National Centers for Environmental Prediction aviation model; the European Centre for Medium-Range Weather Forecasts (ECMWF) spectral model; and the global version of MM5] reproduced conditions in the free atmosphere with good skill. Overall, the ECMWF model performed the best of any of the models, and the authors attributed this to its relatively high resolution near the pole and its high quality initial conditions.

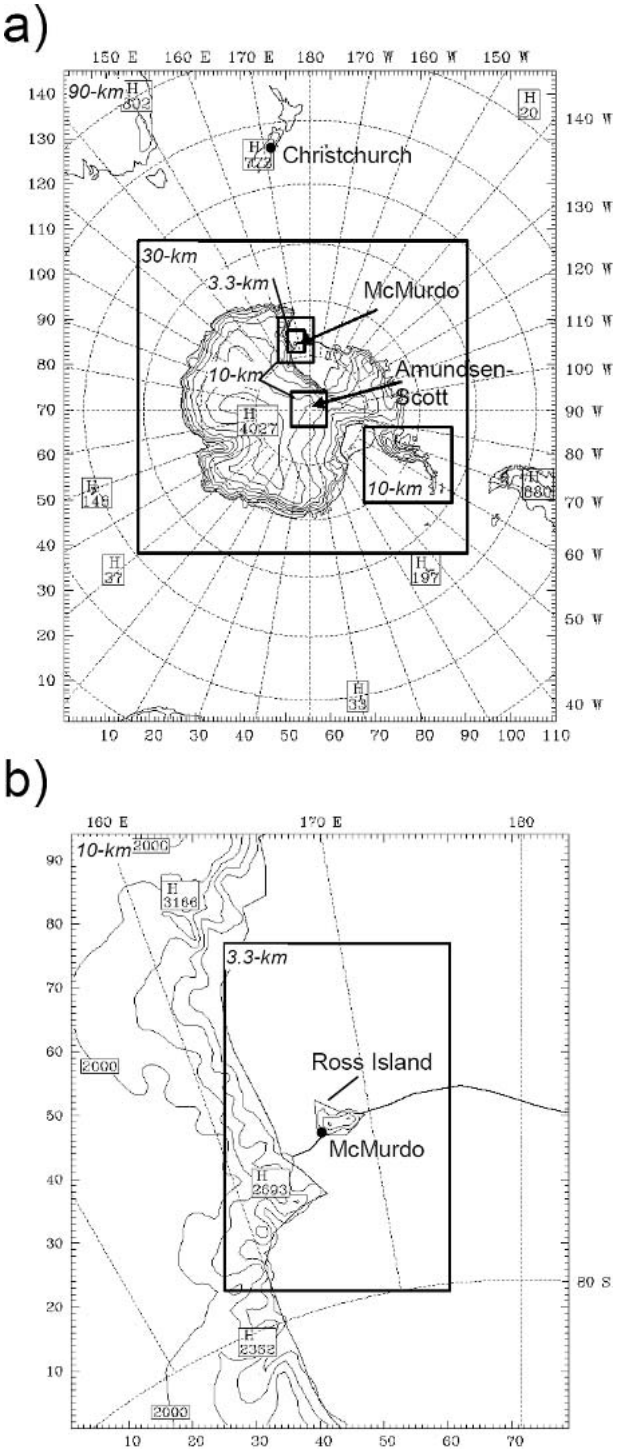

FIG. 1. (a) The AMPS 90-, 30-, 10-, and 3.3-km domains and (b) an enlarged view of the AMPS 10- and 3.3-km domains in the McMurdo region.

Near the surface the simulations had considerably lower skill and more variability between the models, with the highest-resolution models performing best (even at the pole, where the topography is not com-

plex). The lower skill, regardless of resolution, suggests that the planetary boundary layer (PBL) parameterizations currently employed do not adequately represent the near-surface polar atmosphere.

Mesoscale atmospheric models (also called limited-area models) have been used extensively to model various features of Antarctic weather and climate for offline scientific investigations (e.g., Gallée 1998; van Lipzig et al. 2002; Bromwich et al. 2004; Parish and Cassano 2003; Renfrew 2004). However, until recently, real-time forecasting in the Antarctic has been limited to relatively low resolution global models that are optimized for midlatitude applications [Pendlebury et al. (2003) present a thorough evaluation of the performance of these models]. This has changed in the past few years, with at least two other real-time Antarctic mesoscale models being used in addition to AMPS. One of these is a standard version of MM5 run by the U.S. Air Force Weather Agency at 45-km horizontal resolution over the continent. The other is the Australian Bureau of Meteorology's Limited Area Predictive System (LAPS; Puri et al. 1998), for which a modified Antarctic version, ALAPS, is run over East Antarctica with a horizontal resolution of 0.25°. An evaluation of ALAPS is given by Adams (2004). The author examined model performance in forecasting extreme wind events at Casey (66.3°S, 110.5°E), oceanic route forecasting over the Southern Ocean, and katabatic flow simulations at Mawson (67.6°S, 62.9°E), and found that ALAPS provided satisfactory guidance for each case.

To date, a comprehensive statistical evaluation of AMPS has not been performed. That is the primary objective of this paper. In section 2, Polar MM5 and the AMPS configuration are covered in more detail. In section 3, data and methods are described. In section 4, a statistical evaluation of the AMPS 30-km domain is presented. In section 5, the higher-resolution 10- and 3.3-km domains over the McMurdo region are examined. In section 6, conclusions are drawn.

2. System configuration

a. Polar MM5 description

A full description of the standard MM5 modeling system is given by Grell et al. (1995). The model employs nonhydrostatic dynamics on an Arakawa B grid. The vertical coordinate system consists of terrain-following sigma levels. Many important changes to MM5 are available in the polar version used here, Polar MM5. These include a modified ice cloud fraction prediction parameterization within the radiation scheme, improved cloud–radiation interactions, an optimized stable boundary layer treatment, improved calculation of heat transfer through snow and ice surfaces, and the addition of a fractional sea ice surface type. These changes are documented in detail in Bromwich et al. (2001) and Cassano et al. (2001). One difference in the Polar MM5 formulation described by Bromwich et al. (2001) and Cassano et al. (2001) and the AMPS Polar MM5 formulation used here is that the Cooper (1986) equation for ice nuclei concentration is used in the explicit microphysics parameterization instead of the equation of Meyers et al. (1992). This was done to be consistent with the formulation in the Reisner 1 microphysics scheme in the MM5 version (V3) that was newer than the version of MM5 used with the development of the original modifications at OSU (V2). Both Meyers and Cooper are alternatives to the Fletcher curve and represent significant improvements over it. The standard MM5 physics options routinely employed by Polar MM5 include the Eta Model PBL scheme (Janjić 1994) and the Grell cumulus scheme (Grell et al. 1995; note that no cumulus scheme is employed on the 3.3-km AMPS grid).

Guo et al. (2003) evaluated a complete annual cycle of 72-h nonhydrostatic simulations at 60-km horizontal resolution over Antarctica and found that Polar MM5 accurately captures both the large- and regional-scale circulation features with generally small bias in the modeled variables. The observed synoptic variability of the near-surface pressure, temperature, wind speed, wind direction, and water vapor mixing ratio, as well as the diurnal cycle of temperature, wind speed, and water vapor mixing ratio are reproduced by Polar MM5 with reasonable accuracy. It is noteworthy that the Guo et al. (2003) study is somewhat similar to this work. However, the objective of that study was to validate the model for a range of time scales from synoptic to annual, focusing primarily on the mean model performance over the continent as a whole. The objective of this study is to validate the model in an operational context, focusing on synoptic time scales and at stations that are of importance to those forecasting weather in the Antarctic. The additional value due to increased horizontal resolution can also be assessed here, as we examine domains ranging from 3.3- to 30-km grid spacing.

b. AMPS configuration

The AMPS Polar MM5 consists of the five polar stereographic domains at the horizontal resolutions described in section 1 and shown in Fig. 1. There are 32 vertical sigma levels, with 11 levels in the lowest 1000 m to capture the complex interactions in the PBL. The lowest half-sigma level is about 13 m above the surface. The model topography is interpolated from a modern 5-km resolution digital elevation model (DEM) for Antarctica (Liu et al. 1999), the RADARSAT Antarctic Mapping Project (RAMP) DEM. The regions spanned by the Ronne/Filchner Ice Shelf and Ross Ice Shelf are specified as permanent ice.

The AMPS Polar MM5 is initialized twice daily at 0000 and 1200 UTC. The initial and boundary conditions are derived from National Centers for Environmental Prediction Global Forecasting System (GFS)

model (this was the "aviation model" prior to March 2002). The GFS first-guess field is objectively reanalyzed with the available observations using a multiquadric technique (Nuss and Titley 1994). The observations available for assimilation include reports from radiosondes, surface SYNOP reports, automatic weather station (AWS) observations, ship reports, and buoys. Satellite-derived cloud-track winds are also assimilated in the 90-km grid. The system ingests sea ice data daily from the National Snow and Ice Data Center for its fractional sea ice depiction.

The model upper boundary condition (UBC) was changed in May 2003 from a rigid lid set at 100 hPa to a nudging UBC set at 50 hPa (with two additional sigma levels) that is adjusted using GFS forecast temperatures in the highest eight sigma levels. The new UBC has made a positive impact on the forecasts, which is discussed in detail in Wei et al. (2004, manuscript submitted to *Mon. Wea. Rev.*).

3. Data and methods

Table 1 summarizes the observational datasets used in this study. Definitions of acronyms that have not previously been defined may also be found in the table. Additional information concerning these data can be found at the Web addresses provided, and some specific details are discussed here.

AWS and manned/upper-air station data are used to examine the quality of Polar MM5 simulations at the surface and in the free atmosphere. Locations of the surface and upper-air stations are shown in Fig. 2, along with the important geographic features mentioned in the text. The data were quality controlled using a standard deviation filter ($\pm 3\sigma$ for surface pressure, geopotential height, and temperature; $\pm 4\sigma$ for wind speed). This generally resulted in only a few outliers being removed from any dataset. Other spurious points were manually removed. Data from the four nearest model grid points are interpolated to the location of each station for comparison. Modeled surface pressure is adjusted to the reported station elevation using the hypsometric equation and the modeled 2-m temperature. Modeled near-surface temperatures and winds are adjusted from the lowest model sigma level (~13 m) to the nominal instrument heights of 2 m (temperature) and 3 m (winds; AWS) or 10 m (winds; manned stations) using Monin–Obukhov similarity theory (Stull 1988). Modeled near-surface temperatures are also adjusted to the reported station elevation using a dry adiabatic lapse rate of $0.01^{\circ}\text{C m}^{-1}$. This is necessary in the coastal regions, as topographic smoothing often causes the model station elevations to be much higher (>100 m) than the reported elevations. Because modeled cloud fields are representative of larger space scales and longer time scales than observed clouds, the observed clouds from manned stations are smoothed by employing a 12-h running mean window; because cloud observations are generally reported at 6 h, this results in the prior and subsequent observation (if available) being averaged in with the current observation. Observations of near-surface atmospheric moisture content (relative humidity or dewpoint temperature) were not available in the archives of manned station data until August 2003, or if they were from AWSs (only a few are equipped to measure humidity), the observations were of questionable quality. Therefore, statistics for near-surface atmospheric moisture are not included in this evaluation. However, upper-air moisture data are included from 850 to 500 hPa. Above this, the air is too cold/dry for reliable humidity observations.

The statistical comparisons of Polar MM5 versus surface and radiosonde observations are compiled from 3- and 6-hourly surface data and 12-hourly radiosonde data. Therefore, the statistics reflect the model performance at synoptic time scales. Statistics are not com-

TABLE 1. Descriptions of the datasets used.

Dataset	Temporal resolution	Typical No. of observations available for a station for Sep 2001–Aug 2003.	Source	Web site
AWS surface observations (pressure, temperature, winds)	3-hourly	~4500	University of Wisconsin Antarctic Meteorological Research Center (AMRC)	http://amrc.ssec.wisc.edu/archive.html
Manned station surface observations (pressure, temperature, winds, cloud fraction)	3- and 6-hourly	~2200	British Antarctic Survey (BAS)	http://www.antarctica.ac.uk/met/metlog/
Manned station radiosonde observations (geopotential height, temperature, dewpoint, and winds)	12-hourly	~800	BAS, AMRC	http://www.antarctica.ac.uk/met/metlog/ http://amrc.ssec.wisc.edu/archive.html

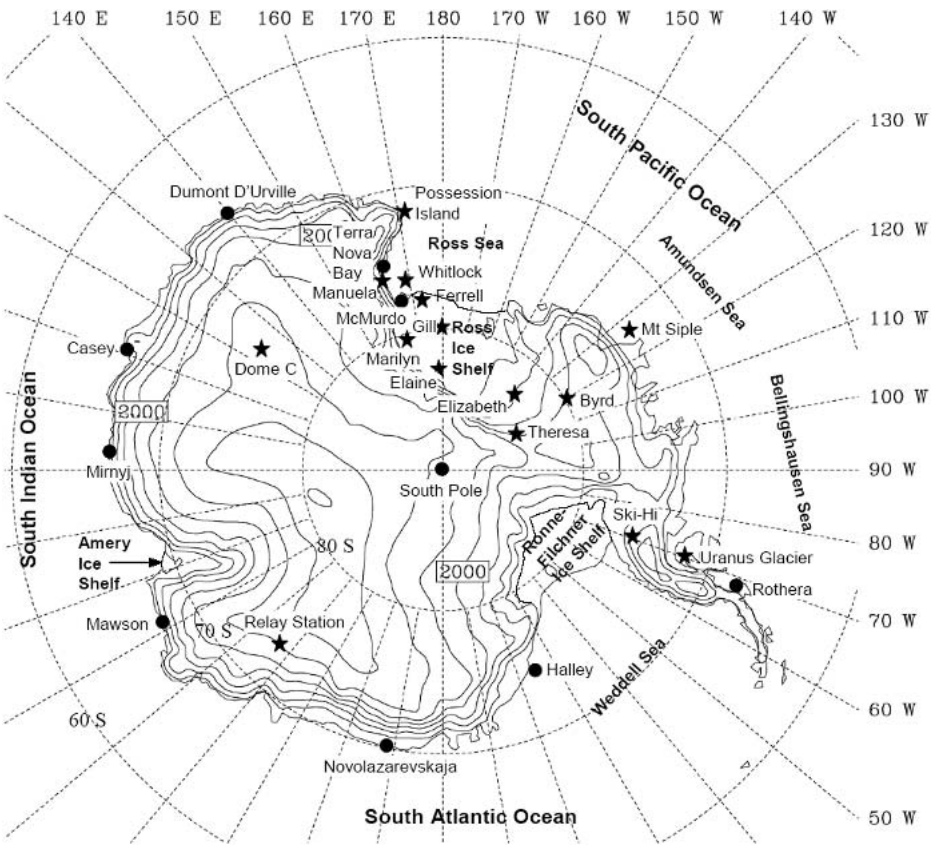

FIG. 2. Names and locations of important geographic features and of AWS (stars) and manned/upper-air stations (circles). Topography is shown at 500-m intervals.

puted when observations are missing. The statistics compiled are bias (model minus observed), normalized root-mean-square (NRMS) error, and correlation coefficient. The NRMS error is the ratio of the rms error to the standard deviation of the observations; this allows the rms errors between sites with different variability to be compared. Here we will consider an NRMS error of 1 to be a "normal" error; an NRMS error <1 will indicate better than normal model performance; and >1 will indicate worse than normal. It is noteworthy that this is an arbitrary scale contrived for the purposes of discussion, and in reality what can be considered satisfactory or unsatisfactory skill is a matter of opinion. The data used to calculate the correlation coefficients were normalized to monthly standardized anomalies $[(x - \bar{x})/\sigma]$ to remove the annual cycle. Correlation coefficients were tested for significance from zero at the 99% confidence level, and in nearly every case passed. The few exceptions are marked in the figures. Weighted means based on the number of observations available at a particular station are used in cases where statistics from several stations are averaged.

It is noteworthy that the statistics presented here are based on observations that are regularly assimilated into the model initial fields. Under the AMPS objective reanalysis package, the model atmosphere will be closer to the input observations at their respective locations at the initialization time. This is a concern, as the statistics may partially reflect the assimilated observations in addition to the model performance. However, as data assimilation theory recognizes, the observations have errors, and also the background fields being reanalyzed have errors. Therefore, even at the initialization time the model does not match the actual atmosphere at an observation location. Additional measures are taken to ensure that the statistics are representative of the model performance by compiling the statistics for forecast hours 12–36, which allows the model 12 h to adjust from the initial fields.

4. Evaluation of the AMPS 30-km domain

In this section, AMPS is evaluated at the surface and upper levels for the 0000 UTC 30-km domain forecasts for the 2-yr period from September 2001 to August 2003. The 1200 UTC forecasts were not extracted because of the limitations of handling the large volume of data (output of one 30-km forecast is >1.6 GB). The statistics are presented in several ways to maximize

their usefulness to the reader. Most of the statistics presented are for variables at 1) the surface and 2) 500 hPa (chosen because it is the first standard pressure level that lies entirely above the surface of Antarctica). Maps of statistics at individual stations show the spatial variability of AMPS skill. Plots of statistics versus month-of-year averaged over many stations indicate the seasonal variability of model skill over the annual cycle. Plots of statistics versus forecast hour averaged over many stations show the degree of degradation (or improvement) of model skill throughout a typical 72-h forecast. Finally, plots of statistics versus pressure level at the two U.S. radiosonde stations indicate the variability of model performance throughout the atmospheric column.

a. Near-surface performance

1) ANNUAL, SEASONAL, AND FORECAST HOUR PERFORMANCE

Figure 3 shows the spatial distribution of the correlation, bias, and NRMS error of AMPS Polar MM5 versus observations for variables at selected surface stations (not all stations are shown because of space limitations). The statistics are calculated for all 12–36-h 0000 UTC forecasts on the 30-km domain over the 2-yr period from September 2001 to August 2003. The 2-m temperature correlations are above 0.8 at most stations except for those in and surrounding the McMurdo region, where they range between 0.5 and 0.8. The biases are negative at most of the coastal stations and slightly positive at the highest elevation (>2000 m) sites (Dome C, Relay Station, and South Pole). Halley Station is an exception to this; a large positive bias is found here. This is likely due to the model depicting Halley as a marine environment rather than that of an ice shelf. The negative biases at most of the coastal sites are partly due to topographic smoothing, which causes the AMPS station locations to be farther inland than they are, and thus depicted as having a more continental environment than is observed. For example, the model surface elevation at Novolazarevskaja, where there is a −3.1°C bias (despite adjusting the temperature for elevation), is 375 m, versus an observed elevation of about 30 m. Higher-than-observed surface elevations are reported at other stations exhibiting negative temperature biases (i.e., Mawson, Mirnyj, Casey, Dumont D'Urville). On the other hand, at Halley, where the warm bias exists, the model surface elevation is 0 m. Surface pressure is represented at all stations with high correlations (>0.9). Biases of surface pressure are strongly dependent on the accuracy of the reported station elevations. The elevations of many of these stations have been determined by aircraft altimeters or guessing (G. Weidner, Antarctic Meteorological Research Center, 2002, personal communication), and therefore they may be in error by more than 100 m (about 12 hPa). For example, this is likely the case at Ski-Hi, where the bias is >20 hPa (S. Colwell, British Antarctic Survey, 2002, personal communication). For this reason the authors have calculated the NRMS error by adjusting the bias to 0 hPa at each site. In this manner, a better estimate of model error can be determined. Small NRMS errors (<0.3) are present at most of the sites [these correspond to unnormalized rms errors (not shown) of about 2–4 hPa].

The modeled near-surface winds are strongly dependent on topography. The (relatively flat) plateau sites tend to have the highest correlations, while sites in mountainous areas (Antarctic Peninsula, McMurdo region) have the lowest correlations. It is also noteworthy that Casey Station (~110°E on the coast), which is directly adjacent to >1000 m Law Dome, has a much lower zonal wind speed correlation than other coastal stations nearby. The winds are too strong at nearly all of the stations; this is especially true along the coast, and inspection indicates that at most stations this is mainly due to the meridional component of the wind. It appears that this results from the location of the coastal stations being farther inland than in reality, and being located on, rather than at the base of, the slopes. Wendler et al. (1993) observed that the strongest winds are some distance inland from the coast. The largest bias and NRMS errors are at Dumont D'Urville (~140°E on the coast), which is located in a region noted for its persistent katabatic wind regime (Periad and Pettré 1993). An even more prominent area of intense katabatic outflow lies just to the east of Dumont D'Urville (Wendler et al. 1997), confirmed by AWS observations at Cape Denison (142.7°E). Plots of the modeled wind speed (not shown) place this wind speed maximum farther westward, near Dumont D'Urville. Thus, the large wind speed bias at Dumont D'Urville may be due to this displacement. Wendler et al. (1993) present MM5-like simulations of the wind field in this region and encountered the same issue. Wind speeds were overestimated at Dumont D'Urville and were underestimated at Cape Denison. In any case, a high-resolution model grid may be desirable if real-time numerical weather prediction in support of aircraft operations were considered for this region.

Figure 4 shows the annual cycle of correlation coefficient, bias, and NRMS error for the AMPS 12–36-h forecast surface variables averaged over all stations at elevations below 500 m (coastal stations; 14 total). A similar plot for stations with elevations above 500 m is included in the appendix (Fig. A1). In general, model simulations for 2-m temperature, surface pressure, and 3-m winds are slightly better at the stations above 500 m. For 2-m temperature, lower correlations, higher NRMS errors, and more negative biases are present in the summer months. This appears to be mainly due to the topographic smoothing mentioned above; in the summer, this effect would be amplified because of the larger land/sea temperature contrast that results from reduced sea ice. It also is likely in part due to the mod-

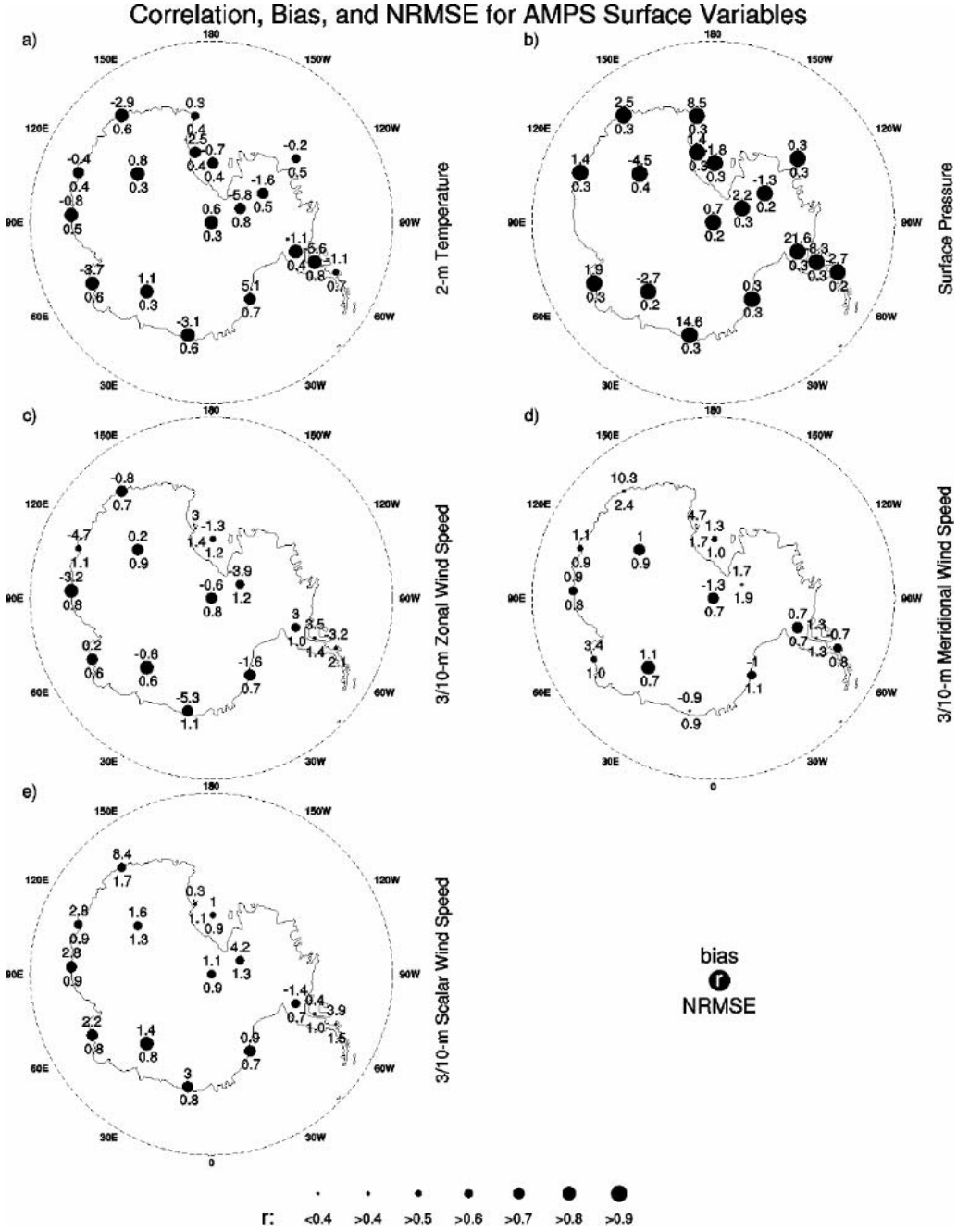

FIG. 3. Correlation coefficient (dot), bias (top number; units given below), and NRMS error (bottom number; dimensionless) at selected Antarctic stations for (a) 2-m temperature (°C), (b) surface pressure (hPa), (c) 3- (AWS) and 10-m (manned) zonal wind speed (m s^{-1}), (d) 3- and 10-m meridional wind speed (m s^{-1}), and (e) 3- and 10-m scalar wind speed (m s^{-1}). The statistics are calculated for hours 12–36 for all 0000 UTC AMPS 30-km forecasts for the 24-month period from Sep 2001 through Aug 2003. Bias units are °C, hPa, and m s^{-1} for temperature, surface pressure, and winds, respectively.

el's diurnal cycle, which is examined more closely in section 4a(2), which describes the diurnal cycle. High skill is observed in the surface pressure field year-round. An increase in the surface pressure bias is notable in the spring months; this is not surprising, as these months are known to exhibit the most synoptic variability (e.g., Parish and Bromwich 1997). The model captures the near-surface winds in a fairly consistent manner year-round. Overall, a positive bias that is due mainly to the meridional component (this is largest in

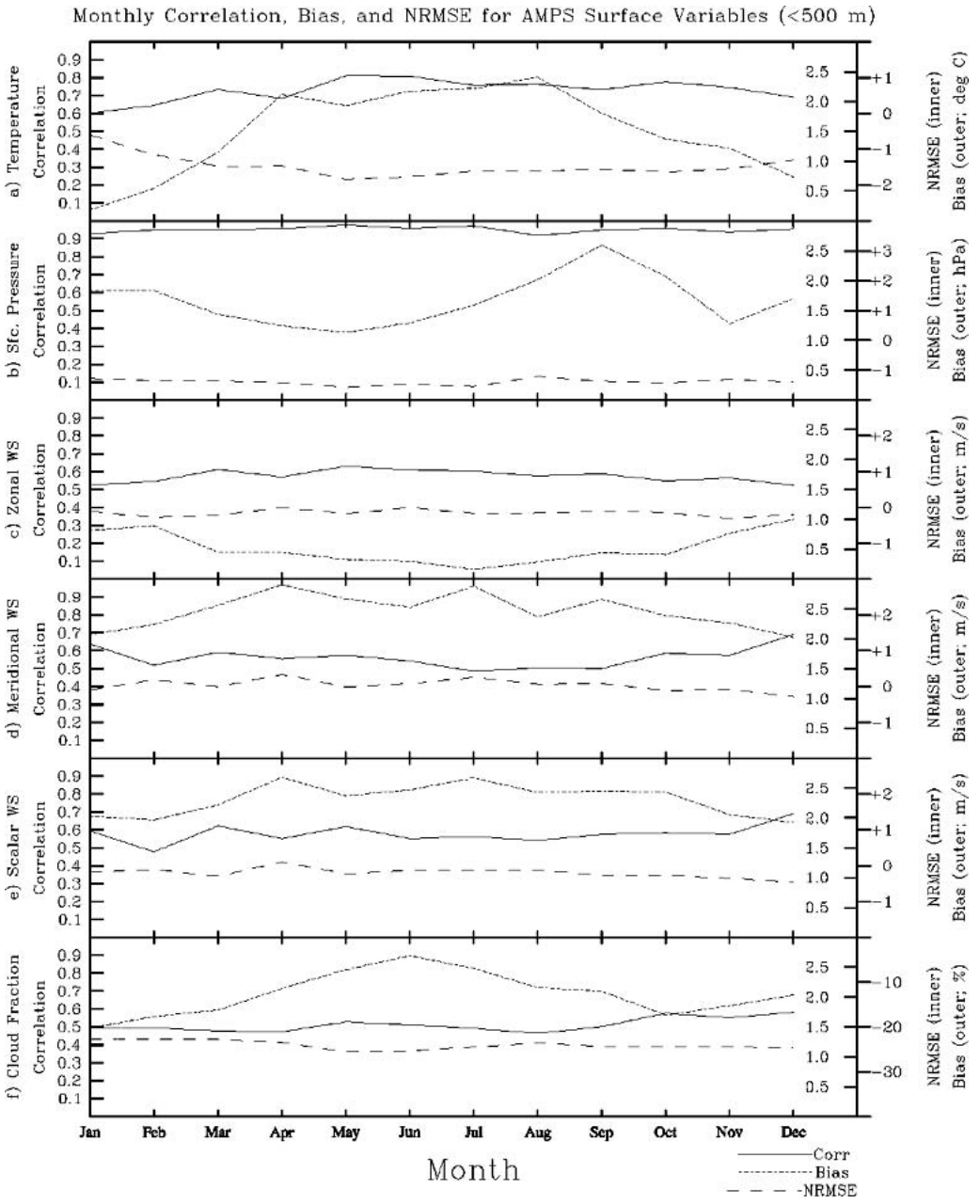

FIG. 4. Annual cycle of correlation coefficient (solid lines), bias (fine dashed lines), and NRMS (dashed lines) error averaged over all Antarctic surface stations below 500-m elevation for (a) 2-m temperature, (b) surface pressure, (c) 3- and 10-m zonal wind speed, (d) 3- and 10-m meridional wind speed, (e) 3- and 10-m scalar wind speed, and (f) cloud fraction. The statistics are calculated for hours 12–36 for all 0000 UTC AMPS 30-km forecasts for the 24-month period from Sep 2001 through Aug 2003.

the winter) is present; as with the negative temperature bias, this appears to be partially due to topographic smoothing. This was confirmed by plotting the soundings of modeled versus observed near-surface temperature and winds at Mawson (not shown) for the modeled station location (inland from the coast at about 317 m ASL) and for a nearby point just off the model coast (at sea level). The modeled inversion and meridional winds were both much weaker at the point just off the coast, and were closer to the observations in the lowest 200–400 m of the atmosphere. However, inspection of the soundings also indicated that the wind speeds appear to be too strong throughout the troposphere. This indicates that other factors may contribute to the wind speed bias; because of the complexity of this issue, it is reserved for investigation in a follow-on paper.

The model shows less skill at simulating clouds, but the correlations are all significantly different from zero at the 99% confidence level. Because the model does not explicitly predict it, cloud fraction (CF) is calculated as the integrated cloud optical depth τ adapted from the Community Climate Model Version 2 (CCM2) radiation scheme that is employed by Polar MM5 (Hack et al. 1993),

$$\mathrm{CF} = \tau = \int_{\sigma=1}^{\sigma=0} [0.1(\mathrm{CLWP}) + 0.0735(\mathrm{CIWP})]\, d\sigma, \tag{1}$$

where CLWP is cloud liquid water path and CIWP is cloud ice water path at each ½ sigma level, and the 0.1 and 0.735 are longwave absorption coefficients. Cassano et al. (2001) describe how cloud liquid and ice water are determined in Polar MM5. Correlations are about 0.5–0.6, but NRMS errors are large [>1; unnormalized rms errors (not shown) are >35%], and a negative bias is observed year-round (largest in the warmest months). Guo et al. (2003) attributed this to a low-level dry bias and to the manner in which cloud optical depth is calculated (the selection of absorption coefficients introduces uncertainty). Using cloud optical depth as a proxy of cloud fraction also introduces uncertainty, but the correlation coefficients suggest this method provides at least a qualitative estimate of cloud variability.

Figure 5 shows the correlation coefficient, bias, and NRMS error versus forecast hour averaged over all Antarctic surface sites. The correlation coefficients and NRMS errors degrade nearly linearly for the variables as the forecast progresses. The exception to this is surface pressure, for which the correlation coefficient, bias, and NRMS errors improve in the first 12 h of the forecast (bias continues to improve throughout the forecast). Experience shows that most of this adjustment is concentrated in the first few hours, which is not evident in the 12-h intervals employed here. This likely reflects dynamical imbalances existing in the model's initial conditions. For example, the model must initialize surface pressure based on the mean sea level pressure (MSLP) field from GFS (no surface pressure field is available); this can cause large biases over the high continental interior where large inversions are common, hindering the extrapolation technique. This was partially alleviated by modifying the algorithm that estimates surface pressure hydrostatically from MSLP (Manning and Powers 2002). The modified algorithm uses a time-averaged value for surface temperature rather than an instantaneous value of temperature from a pressure level near the surface. The latter caused a positive surface pressure bias on the order of tens of hectopascals over the highest elevations because the pressure level was above the inversion. It is also possible that the model is making adjustments from other initial synoptic fields. Considerable changes from the initial conditions are also evident in the wind and temperature fields, as the most rapid changes in biases and rms errors occur in the first 12 h of the forecast, though these are characterized by decreases in model performance. Similarly, Bromwich et al. (2003) and Monaghan et al. (2003) note the strong sensitivity of AMPS to the initial fields.

2) DIURNAL CYCLE

To evaluate the diurnal cycle in AMPS, Figs. 6 and 7 present the monthly time series of observations versus Polar MM5 12–36-h simulations for January 2003 at Mawson (16 m ASL) and Relay Station (3353 m ASL). Mawson is typical of the research stations that dot the coastal margins of Antarctica, while Relay Station is representative of the high-elevation plateau environment. Twenty-four-hour daylight persists through 12 January at Mawson, and throughout all of January at Relay Station. At Mawson (Relay Station) the clear-sky incoming solar radiation on 15 January is about 940 W m^{-2} (840 W m^{-2}) at solar noon, and the daily mean is about 410 W m^{-2} (440 W m^{-2}). Figures 6e and 7e show the average diurnal cycles of temperature and wind speed for the month. At Mawson, the model temperature bias is small (−1°C) for the daytime high, but much larger (−4° to −5°C) for the nighttime low (Figs. 6a and 6e). As noted earlier for the cold bias observed in the coastal regions during summer (Fig. 4a), this is thought to be caused by a more continental (rather than marine) representation of coastal stations due to topographic smoothing along the continental margins, which likely amplifies the model diurnal temperature cycle; the elevation of Mawson in AMPS, interpolated from the four nearest grid points, is about 317 m. At Relay Station the model temperature bias is small (<|1°C|) over the entire diurnal cycle (Figs. 7a and 7e).

Surface pressure is simulated with good skill at both stations; at Relay Station, the modeled pressure has subtle diurnal oscillations that are not present in the observations. Although some of these oscillations result from the reinitialization of the model each day, most occur within the forecasts; this may be caused in part by the diurnal temperature cycle affecting the reduction of the modeled station elevation to the observed station elevation when processing the data for this comparison. This may also be partly due to the modeled surface pressure adjusting from the surface pressure in the initial conditions, which must be extrapolated from the GFS MSLP field and is known to be biased at high elevations (Manning and Powers 2002). However, this latter adjustment is usually only present in the early hours of the forecast and is mostly damped in the 12–36-h output plotted in Figs. 6 and 7. There is also a persistent negative bias. This could be due to an error in the reported AWS elevation to which the model pressure is adjusted. However, at another high plateau station, Dome C (3250 m ASL; not shown), there is a similar negative bias. This may be due to a problem

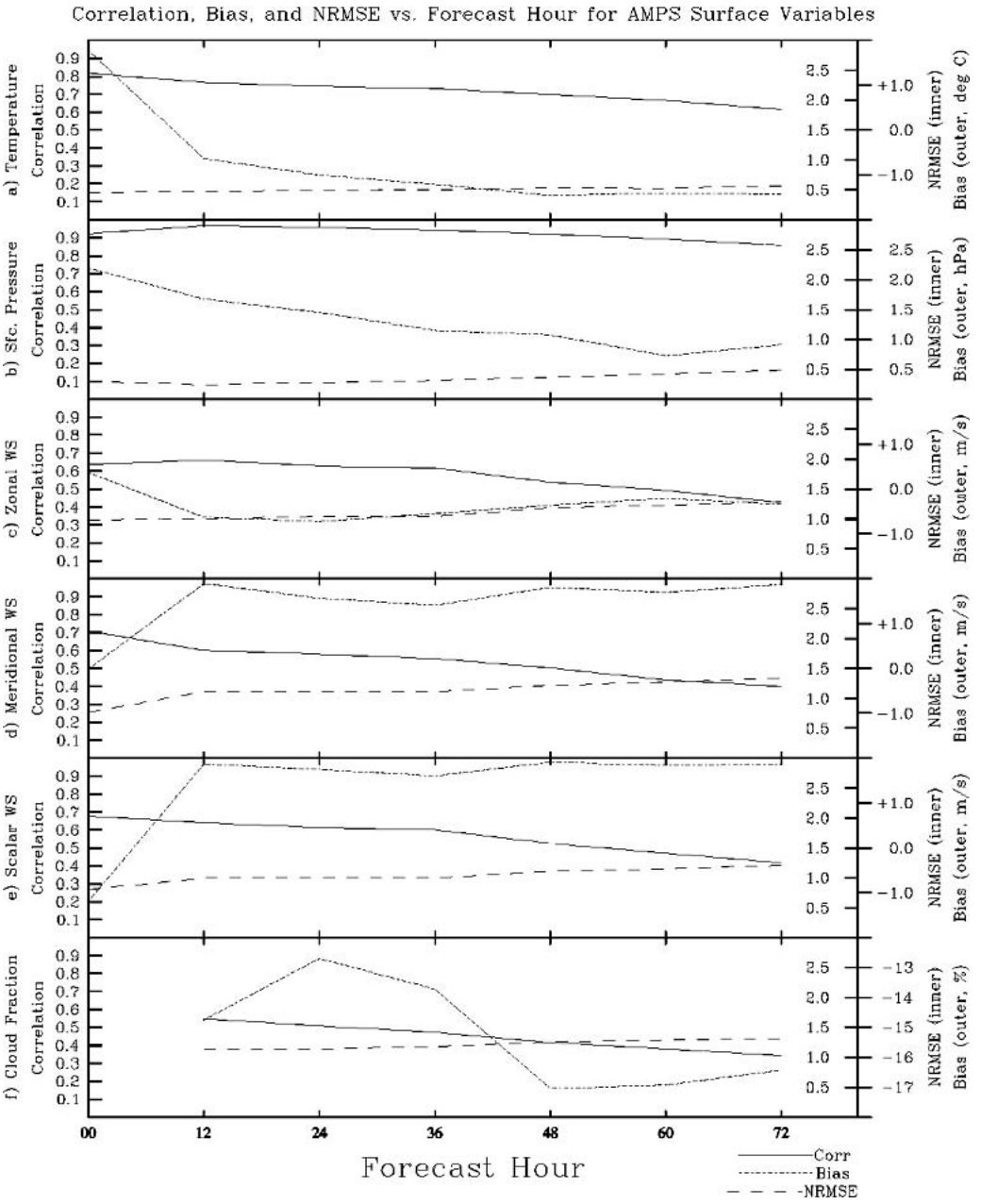

FIG. 5. Correlation coefficient, bias, and NRMS error vs forecast hour averaged over all Antarctic surface stations for (a) 2-m temperature, (b) surface pressure, (c) 3- and 10-m zonal wind speed, (d) 3- and 10-m meridional wind speed, (e) 3- and 10-m scalar wind speed, and (f) cloud fraction. The statistics are calculated for all 0000 UTC AMPS 30-km forecasts for the 24-month period from Sep 2001 through Aug 2003.

with the model's mass loading over the continental interior; however, there are no radiosoundings at Relay Station or Dome C to compare with the modeled tropospheric temperatures. At the only interior station with regular radiosonde observations, South Pole, the model has a $\sim -2°C$ cold bias throughout the column. Actually, this should lead to a 6-hPa *positive* surface pressure bias; however, there is no surface pressure bias present at South Pole. Other plateau stations at lower elevations (below 3000 m) do not exhibit large surface pressure biases either. Therefore, this problem, which is present year-round, appears to be constrained to only the highest elevations over East Antarctica. The detailed analysis required to properly resolve this issue is reserved for a follow-on study.

The maximum daily wind speed occurs at approximately the time of coolest temperature at Mawson, in agreement with the observations (Figs. 6a, 6c, and 6e).

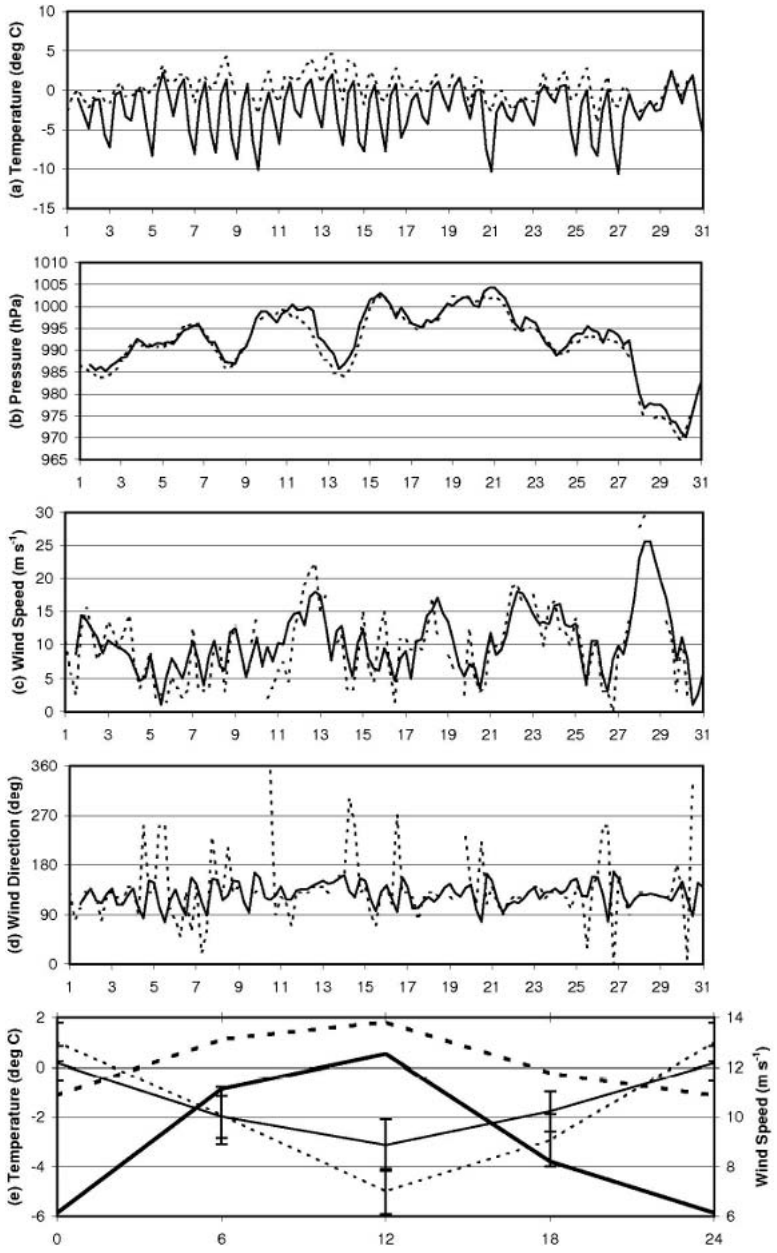

FIG. 6. (a)–(d) Monthly time series (UTC) of 6-hourly station observations (thin dashed lines) and Polar MM5 12–36-h simulations (thin solid lines) at Mawson for Jan 2003 for (a) 2-m temperature (°C), (b) surface pressure (hPa), (c) wind speed (m s^{-1}), and (d) wind direction (°). (e) Diurnal cycle of 6-hourly station observations (dashed lines) and Polar MM5 12–36-h simulations (solid lines) for Jan 2003 for temperature (thick lines; °C) and wind speed (thin lines; m s^{-1}). Error bars are shown in (e) for wind speed, and represent $\sigma/\sqrt{n}$. Local time is on the x axis in (e), i.e., "12" corresponds to local noon.

By contrast, at Relay Station, the maximum wind speed occurs at approximately the time of the maximum temperature (Figs. 7a, 7c, and 7e). The winds at Mawson appear to be subject to buoyancy (katabatic) forcing at night due to an inversion, and to the large-scale pressure gradient forcing during the day once the inversion breaks down (e.g., Kodama et al. 1989; Bintanja 2000). This is supported by the wind direction observations, which are more variable during the day. At Relay Station, the near-simultaneous timing of the peak wind speed with the maximum daily temperature suggests that the behavior of the near-surface winds is due to

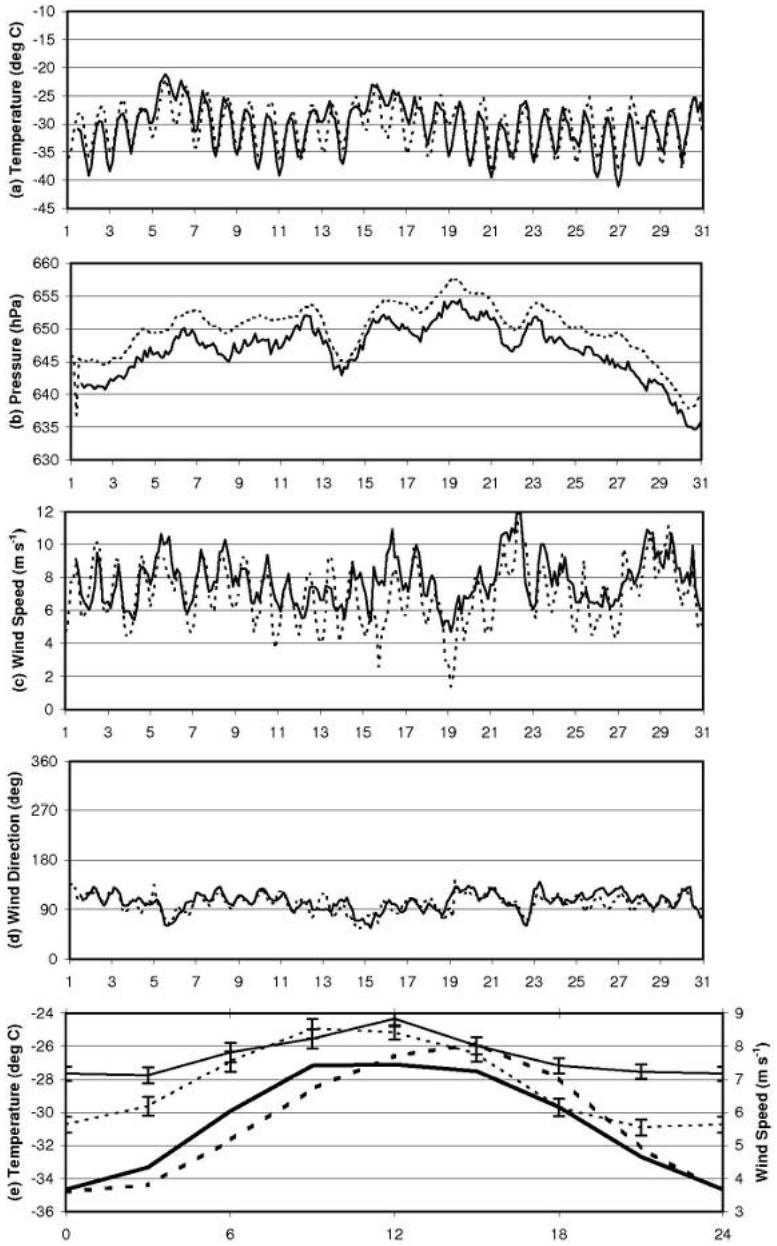

FIG. 7. Same as 6, but for 3-hourly data at Relay Station.

momentum transfer as the stable boundary layer heats up and higher momentum air aloft mixes downward (as is commonly observed at midlatitudes).

At Mawson, the model overpredicts the daytime wind speed minima (although the error bars suggest this may not be significant), but predicts the nighttime maxima with good skill. At Relay Station, the daytime maxima are simulated with good skill, but the nighttime minima are too strong. Recall from above that at Mawson, the nighttime near-surface temperature bias is large, while at Relay Station, it is small. When considered in conjunction, these observations suggest that there is not enough drag acting on the surface wind. To explain, at Mawson, a large nighttime cold bias (i.e., excessive near-surface stability) is required to slow the modeled wind speed enough so that it matches the observations. At Relay Station, where there is a negligible nighttime temperature bias (i.e., approximately correct near-surface stability), the winds are too strong. Therefore, it may be relatively straightforward to correct this problem by increasing the surface roughness in future releases of the model (currently it is set at 0.10 mm). This is not an unreasonable assumption, considering roughness length observations over snow and ice vary

widely and are often larger than the value used in AMPS. For instance, Budd et al. (1964) measured values from about 0.05 to 0.5 mm at Byrd Station depending on wind speed and snow conditions. Weller (1968) measured values from 0.14 mm (gentle snow covered slopes) to 2.6 mm (coastal ablation zone). More recently, Bintanja and van den Broeke (1995) measured values ranging from 0.08 to 0.75 mm; the higher values were measured at sites with sastrugi (snow ridges). In view of this large range of values, it may also be useful to implement a variable surface roughness scheme.

The wind direction is well simulated at both sites, although the observed winds at Mawson are more variable than the modeled winds. It may be that the modeled inversion layer at Mawson is not breaking down to the extent that it is in reality; this is suggested by the modeled wind speed, which is slightly too strong during the day. Inspection of modeled versus observed atmospheric soundings (not shown) at Mawson for January 2003 support this, indicating more instability in the layer immediately adjacent to the surface during daytime than is simulated by AMPS. Again, it is noteworthy that this is at least in part due to the model topography near Mawson, where a considerable variability in winds has been observed over relatively small space scales (Adams 2004). Wind speeds representing a 30 km $\times$ 30 km model grid box are being compared to observations at a single point, and one might expect the observations to be more variable. Comparison of modeled and observed soundings at South Pole for January 2003 (not shown), where topography is less variable, shows that the modeled and observed temperature and wind fields at low levels are in good agreement.

b. Upper-level performance

For brevity, much of the 500-hPa statistical analysis is included in the appendix. (Figures A2, A3, and A4 are similar to Figs. 3, 4, and 5, but for 500-hPa temperature, geopotential height, zonal wind speed, meridional wind speed, scalar wind speed, and dewpoint temperature.) Although a detailed discussion is omitted here, it is noteworthy that the model skill is higher in the free atmosphere than at the surface, in the absence of topographic effects. Temperature and geopotential height are characterized by correlation coefficients >0.9, and small biases and NRMS errors. Winds are characterized by correlations >0.8 for the zonal and meridional components, and >0.7 for the scalar winds. Dewpoint temperatures, which are not evaluated at the surface, are simulated with lower skill than for other variables. There is generally a positive model bias, indicating the column is too moist at 500 hPa. NRMS errors are also larger for dewpoint temperatures than for other variables [unnormalized rms errors (not shown) are about 5°–7°C]. This may be due in part to the air being very dry in an absolute sense at 500 hPa, and therefore small errors in simulated moisture can lead to large errors in dewpoint temperature. For example, at 500 hPa a 0.01 g kg^{-1} change in water vapor mixing ratio corresponds to a 5°C change in dewpoint at temperatures close to −40°C. This bias may also be due in part to measurement errors. Recent tests of Vaisala RS80 sondes at Dome C (also used at South Pole since August 2001) suggest problems as well; the response time of the relative humidity measurements to changes in temperature is slow, especially in winter (Hudson et al. 2003).

Figures 8 and 9 show the correlation, bias, and NRMS error for the atmospheric soundings at two U.S. Antarctic stations, McMurdo and Amundsen-Scott. The statistics are calculated for all 12–36-h 0000 UTC forecasts on the 30-km domain over the 2-yr period from September 2001 to August 2003. McMurdo represents a coastal environment in an embayment (covered by sea ice much of the time), while Amundsen-Scott represents the plateau environment at South Pole. Note that the McMurdo soundings extend from 150 down to 850 hPa, while the Amundsen-Scott soundings extend from 150 down to 500 hPa because of the elevation of the South Pole (2835 m ASL). Comparison indicates that the model performance throughout the atmospheric column at McMurdo and South Pole is qualitatively similar. Temperature correlations are consistently about 0.8 throughout the atmosphere at both stations. Temperature biases are small and become generally warmer and slightly positive near the tropopause (~300 hPa). Geopotential height correlations are high ($r > 0.95$) throughout the atmosphere, accompanied by small biases and NRMS errors. Zonal winds are captured with the best skill in the free atmosphere; below 500 hPa model skill drops off sharply at McMurdo because of the complex topography. This drop-off in skill is not as marked in the near-surface meridional winds because of the persistent low-level southerly wind regime that is characteristic along the Transantarctic Mountains (e.g., Seefeldt et al. 2003). At McMurdo, the zonal and meridional wind biases become more negative with height in the atmosphere, although the zonal biases become smaller, while the meridional biases become larger. At South Pole, the biases generally become more positive with height, especially above the tropopause. Overall, the scalar wind speed has correlations between 0.7 and 0.8 throughout the atmosphere, and biases are small ($<\pm 1$ m s^{-1}). Biases and NRMS errors for dewpoint temperature increase sharply with height; the possible reasons for this are discussed above and are likely related to low absolute humidity and instrumental biases.

In summary, AMPS performs remarkably well at both the surface and in the free atmosphere. The diurnal cycle of near-surface temperature, pressure, wind speed, and direction are reasonably captured by the model. However, systematic and interrelated tempera-

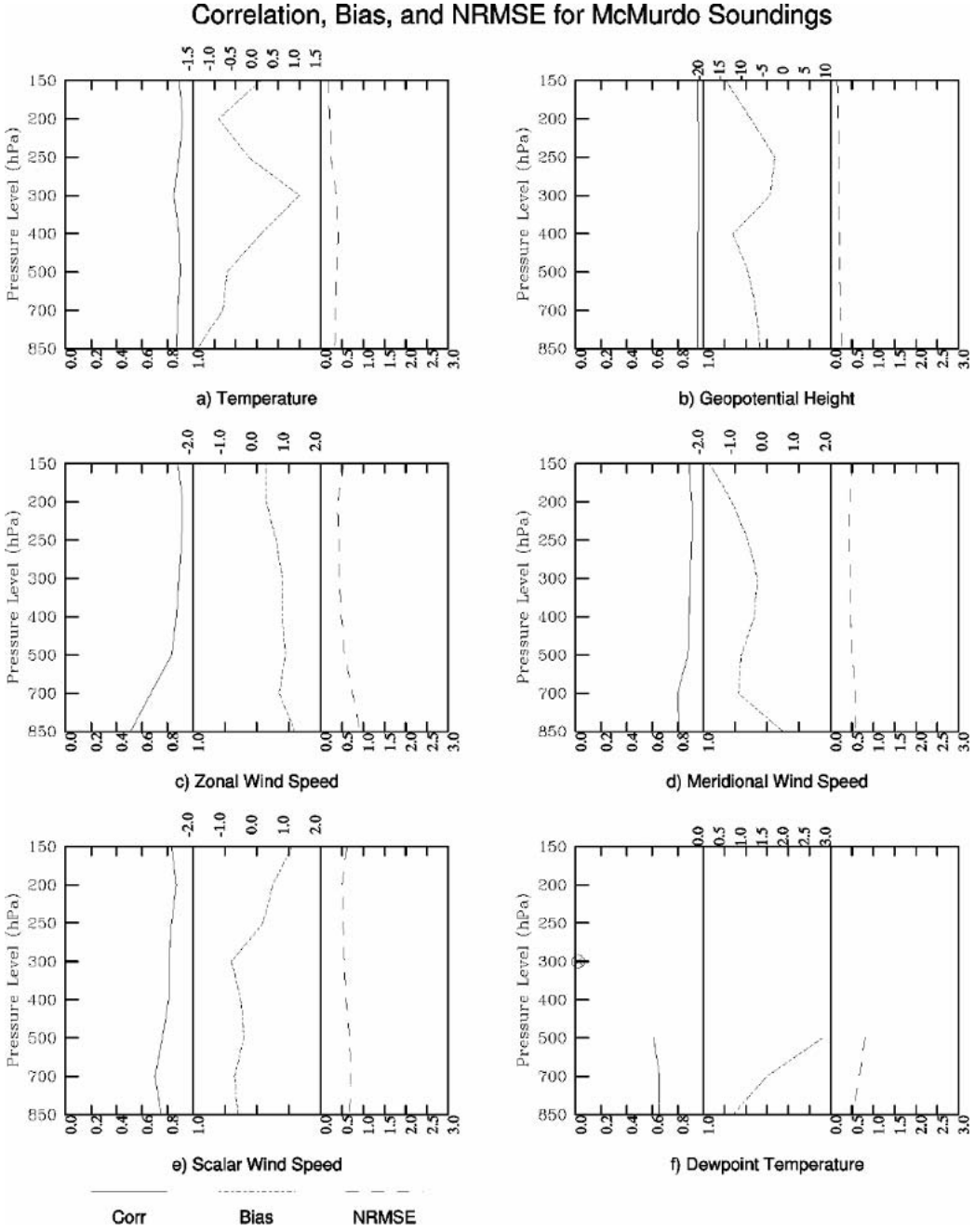

FIG. 8. Correlation coefficient, bias, and NRMS error vs height at McMurdo Station for (a) temperature, (b) geopotential height, (c) zonal wind speed, (d) meridional wind speed, (e) scalar wind speed, and (f) dewpoint temperature. The statistics are calculated for all 0000 UTC AMPS 30-km forecasts for the 24-month period from Sep 2001 through Aug 2003. Bias units are °C, m, and m s^{-1} for temperature (and dewpoint temperature), geopotential height, and winds, respectively.

ture and wind speed biases are present during certain times of day. Uniformly increasing the surface roughness in the model, or implementing a variable surface roughness scheme, may be the most efficient approach toward solving this problem. Regionally, there does not appear to be any sector of Antarctica that has better/poorer performance than any other sector, although strong dependence on topography is noted near the surface, with poorer model performance in regions of large topographic variability. Little change in model skill is noted over interseasonal time scales. Adjustments occur in the first 12 h of the forecasts from the

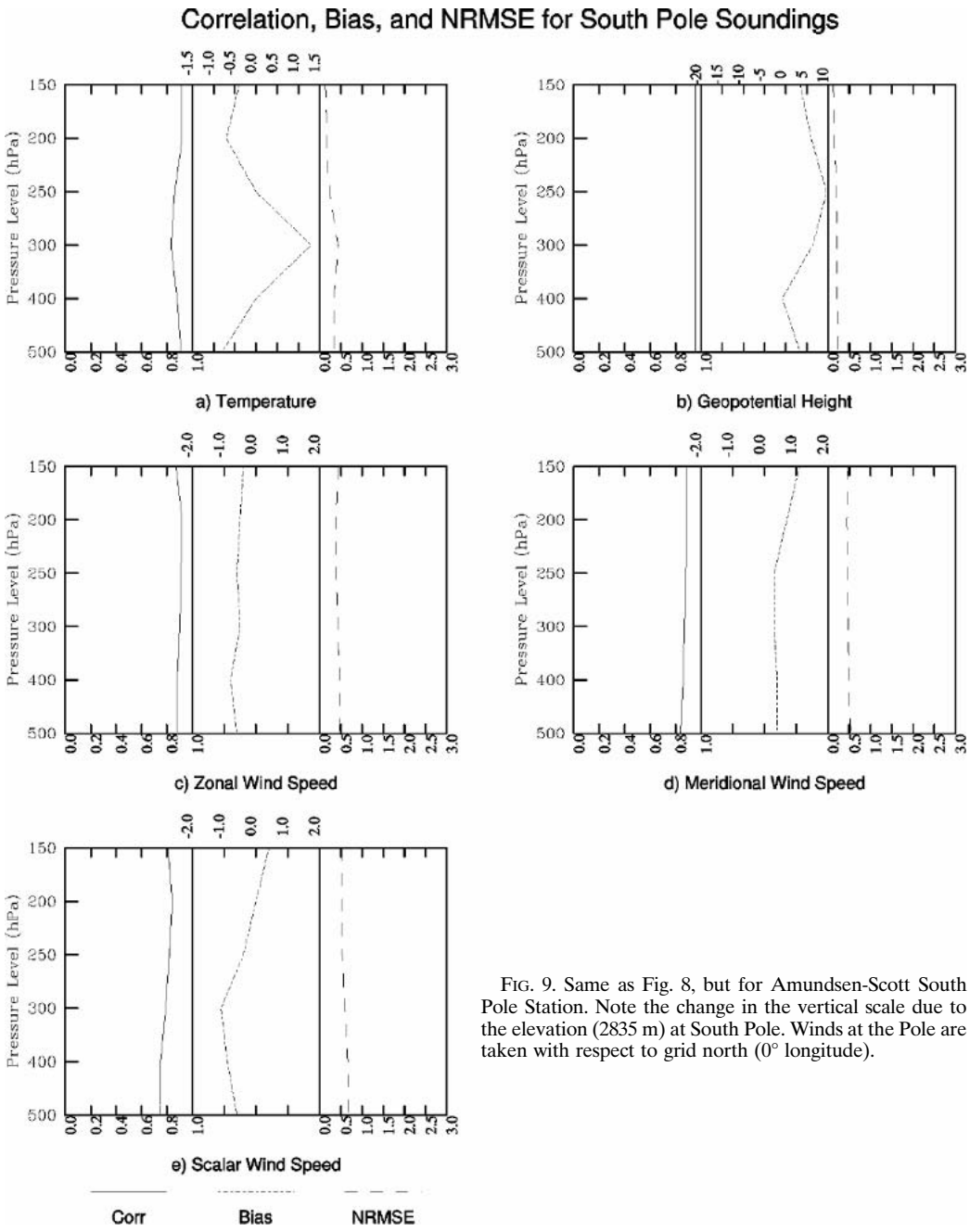

FIG. 9. Same as Fig. 8, but for Amundsen-Scott South Pole Station. Note the change in the vertical scale due to the elevation (2835 m) at South Pole. Winds at the Pole are taken with respect to grid north (0° longitude).

initial conditions. In the following section, the impact of the higher-resolution domains over McMurdo is examined.

5. Evaluation of the AMPS 10- and 3.3-km domains

McMurdo is the hub of the U.S. Antarctic Program's operations, hosting three aircraft runways. The station resides in an area of complex topography, resting on Ross Island at the base of 3794-m Mt. Erebus at the edge of the Ross Ice Shelf (Fig. 10). Two small islands lie immediately to the south, as well as Minna Bluff, an ~1000 m obstacle lying perpendicular to the dominant southerly wind regime that affects the region (e.g., Seefeldt et al. 2003; Fig. 10). The Transantarctic Mountains lie just to the west, across a small sound. Because of the operational importance of McMurdo, the AMPS grid was originally nested to 10-km horizontal resolution over the region. In December 2001, a finer, 3.3-km grid was placed within the 10-km grid. Because of the two-way nesting configuration used in

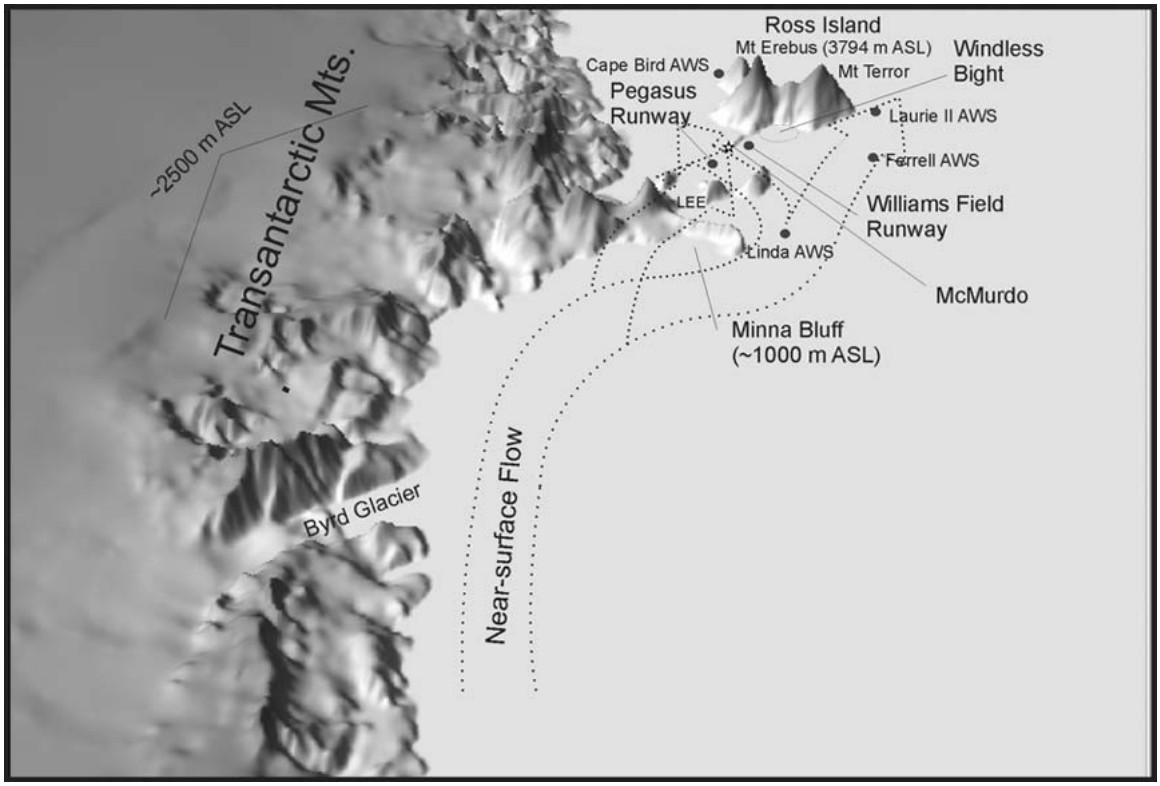

FIG. 10. Topography and geographic features of the McMurdo region. The dominant near-surface flow pattern is also shown. Terrain data are derived from the U.S. Geological Survey (USGS) GTOPO30 dataset. The vertical scale is exaggerated. Adapted from Bromwich et al. (2003).

the AMPS Polar MM5, it is impossible to directly compare the 10-km domain forecasts with those from the 3.3-km domain, as the 3.3-km domain output are smoothed as they are fed back to the 10-km grid; thus the 10-km grid is a smoothed representation of the 3.3-km grid output. However, the subject of whether the 3.3-km forecasts provide enough benefit over the 10-km forecasts to justify the increased computing cost has been a subject of some curiosity. It has been suggested in some instances that the 10-km forecasts may actually provide better guidance than the 3.3-km forecasts, and that perhaps the model physics are not well suited to such fine resolution. To investigate this, NCAR's MMM group ran several months of concurrent AMPS forecasts with the 3.3-km domain turned off along with the real-time AMPS forecasts (which include the 3.3-km grid). In this manner, the 10-km domain and the 3.3-km domain in the McMurdo region can be directly compared for June–July–August (JJA) 2003. We focus on the wind fields, as these are likely to be most sensitive to changes in model resolution.

Figure 11 compares the correlation coefficients for model versus observed zonal (Figs. 11a and 11b) and meridional (Figs. 11c and 11d) wind components on both the 10- and 3.3-km grids. Because the correlation coefficients are taken only at points where AWSs are located, they are kriged[1] to a grid surrounding Ross Island in order to better interpret the regional differences between the domains. It is noteworthy that kriging from a few AWSs (12 total) to an entire grid, especially in regions of complex terrain, does not give a completely accurate depiction of the spatial distribution of correlation coefficients. However, inspection indicates that this technique is adequate for revealing the most important differences between the 10- and 3.3-km grids. Slight improvements are observed on the 3.3-km grid in the zonal wind fields to the north and east of Ross Island. More significant improvements are noted in the meridional winds, evident in Windless Bight (a stagnation zone on the windward side of Ross Island; O'Connor and Bromwich 1988), and especially to the northwest and west of Ross Island. This is important, as the area to the north of the island is a prominent region of frequent mesoscale cyclogenesis (Carrasco et al. 2003). The presence of Ross Island likely plays a role in this process. For instance, Powers et al. (2003) have noted von Kármán vortices forming in the model on the

[1] Kriging is a method of interpolation that assumes the parameter being interpolated can be treated as a regionalized variable. A more detailed description of kriging methods is provided in Davis (1986).

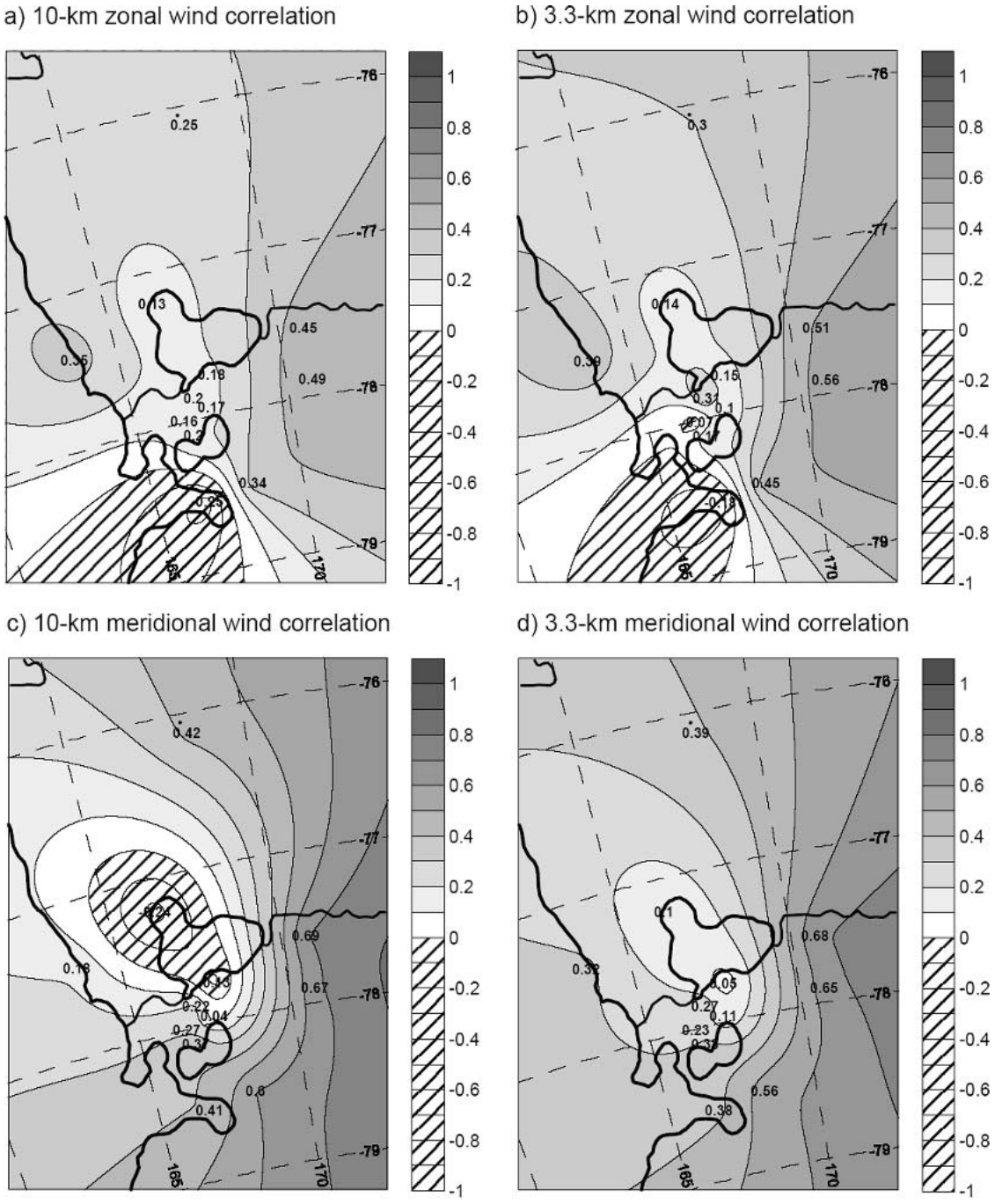

FIG. 11. Correlation coefficients for 10- and 3.3-km domain wind speeds for JJA 2003 for (a) the 10-km zonal component, (b) the 3.3-km zonal component, (c) the 10-km meridional component, and (d) the 3.3-km meridional component. The data are kriged to the grid from the AWS locations [indicated by the correlations shown in (a)–(d)], as described in the text.

lateral sides of the island and drifting toward the north; similar features are present in the satellite imagery. Because of this mesoscale activity, directional constancies in the lee of Ross Island are observed to be lower than in the surrounding areas. Comparing the directional constancies from the 10-km grid and the 3.3-km grid with the observed directional constancies (not shown), it is apparent that the winds on the 3.3-km grid have lower directional constancies than those on the 10-km grid and are in better agreement with the observed values. This indicates that the 3.3-km grid provides a noteworthy enhancement of the wind simula-

tions near Ross Island, an effect that propagates well to the north.

Figure 12 shows the normalized standard deviation of the JJA 2003 wind speed (σ/mean) for the 10-km grid (Fig. 12a), the 3.3-km grid (Fig. 12b), and the ratio of the 3.3-km grid to the 10-km grid (Fig. 12c). A ratio >1 indicates regions where the 3.3-km grid is more sensitive to spatial and temporal changes in the winds than the 10-km grid; the largest values are expected in the areas where the winds are most influenced by the topography. Inspection indicates that the 3.3-km grid is capturing much more detail in the mountainous regions; for instance, resolving both peaks (Mt. Erebus and Mt. Terror) on Ross Island. Figure 12c shows that the 3.3-km grid is more sensitive than the 10-km grid around the periphery of Ross Island and of particular note, in the region to the south of Ross Island where the Pegasus and Williams Field runways reside.

Figure 13 shows the spectral density (unitless) versus frequency (h^{-1}) for JJA 2003 wind speed at two AWS sites near Ross Island for 1-hourly observations, and for 1-hourly output from the 12–36-h AMPS forecasts for the 3.3- and 10-km domains. Spectral density gives a qualitative measure of the amount of energy present at a given frequency. The mean and trend were removed from the data before performing the analysis. An 11-point (0.0046 h^{-1}) Daniell window (centered running mean) was applied to the periodogram to facilitate plotting. The AWS sites were chosen because of their close proximity to the topography of Ross Island. At Williams Field, topographic influences are strong, and one would expect important differences between the 3.3- and 10-km domains. Inspection indicates that there is more energy present in the 3.3-km domain than the 10-km domain at high frequencies (short time scales), and that this is in good agreement with observations. At Cape Bird, the differences between the domains are not as prominent, but the 3.3-km domain still exhibits more energy at high frequencies, which is in agreement with the observations. At locations farther east of Ross Island that are not as prone to topographic influences, there is little difference between the 3.3- and 10-km domains (not shown).

Based on the findings above, it is clear that the model physics are still valid at 3.3-km resolution and that this grid provides an improved depiction of the near-surface winds in the McMurdo region. Realistically, the improvement in skill is not as great as expected; it is anticipated that ongoing efforts to upgrade the model numerics by implementing a higher-order finite-differencing scheme for the calculation of the horizontal pressure gradient force will lead to further improvements to the 3.3-km grid.

6. Conclusions

Calculated over 2 yr of forecasts, the 12–36-h near-surface temperatures typically have correlation coefficients exceeding 0.75, with negative biases at the coast and at the lower-elevation plateau stations, and slightly positive biases in highest areas (>2000 m) of the continental interior. Over the annual cycle, surface temperature simulations are best in the winter months. Surface pressure is very well simulated; correlations are typically greater than 0.95 over the entire annual cycle. On average, the pressure biases are +1–2 hPa, and NRMS errors are usually <0.3. The modeled winds are strongly dependent on topography, with the relatively flat plateau stations having the higher correlation coefficients for wind speed (~0.6–0.7) than the coastal stations (~0.5–0.6). A positive bias of 1.5–2 m s^{-1} (largest in winter) is present in the coastal regions and is attributable mainly to the meridional component of the wind; this is in part due to topographic smoothing, which causes coastal stations to be located farther from the ocean in the model than in reality, where the winds are stronger. Topographic smoothing causes systematic biases in nearly all of the near-surface modeled fields for coastal stations, and it should be considered when con-

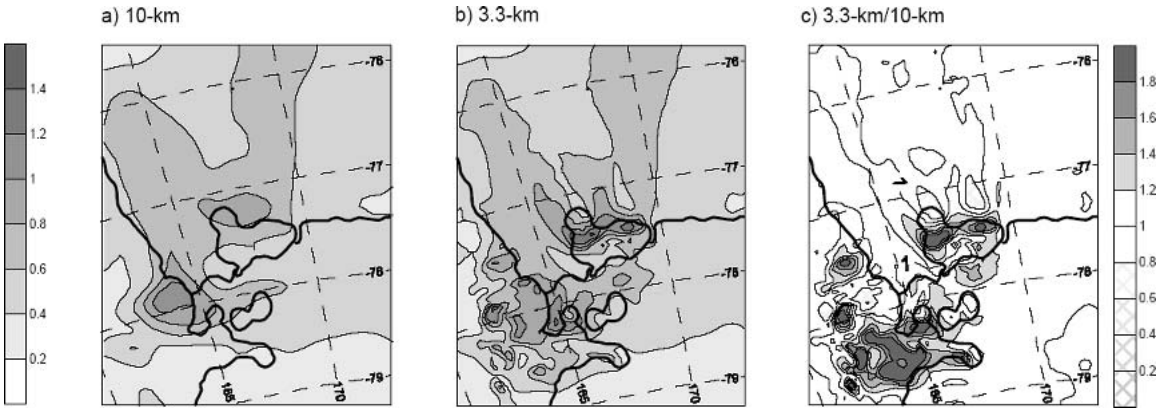

FIG. 12. The normalized standard deviation of the JJA 2003 wind speed (σ/mean) for (a) the 10-km grid, (b) the 3.3-km grid, and (c) the ratio of the 3.3-km grid to the 10-km grid. The left-hand scale applies to (a) and (b). The right-hand scale applies to (c).

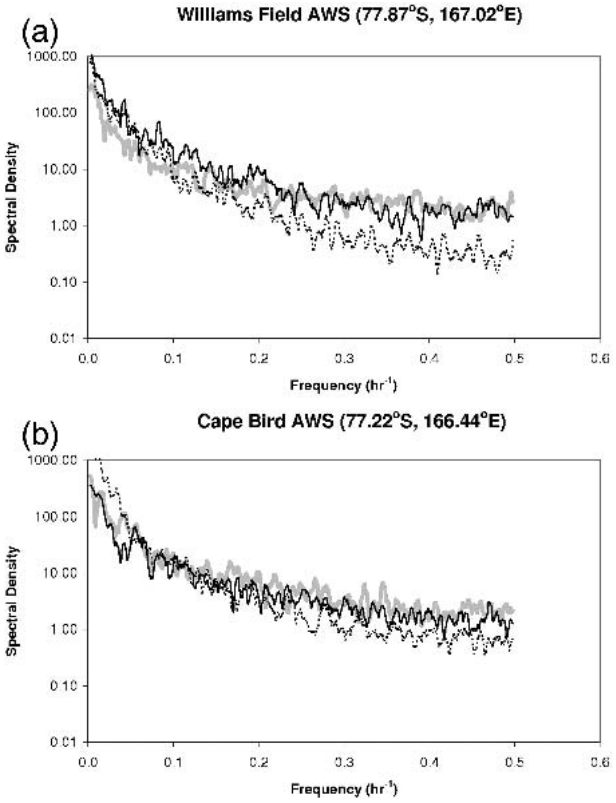

FIG. 13. Spectral density (unitless) vs frequency (h^{-1}) for JJA 2003 wind speed at two AWS sites near Ross Island for observations (thick gray), the 3.3-km AMPS domain (solid black), and the 10-km AMPS domain (dashed black). The analyses were applied to 1-hourly data; the AMPS data are from the 24–36-h forecasts. The mean and trend were removed from the data before performing the analysis. An 11-point (0.0046 h^{-1}) Daniell window (centered running mean) was applied to the periodogram to facilitate plotting.

structing time series products for AMPS real-time forecasts; perhaps relocating the points nearer the model coastline would provide more realistic guidance. Cloud fraction is simulated with marginal skill; correlation coefficients are about 0.5 over the annual cycle, and NRMS errors are ~1. The clouds are underpredicted by about 10%–20% along the coast; the negative bias is most notable on the polar plateau and largest in the warm months. This bias, however, appears to be largely due to the use of cloud optical depth as a proxy of cloud fraction, as the dewpoint temperature biases in the troposphere do not suggest an undersimulation of the moisture in the atmospheric column. Modifying or tuning this algorithm for Antarctic cloud conditions is planned. Generally speaking, cloud estimates are better than expected, especially considering the highly variable nature of cloud fraction observations.

The AMPS Polar MM5 near-surface skill with respect to forecast hour generally decreases linearly as the forecasts progress from hour 00 to hour 72, except in the surface pressure field, for which the skill increases for the first few hours. This is due in part to initialization errors caused by estimating surface pressure from the GFS sea level pressure field over the cold, high Antarctic terrain. Rapid adjustments in the temperature and wind fields are also observed in the first few hours of the forecast.

The diurnal cycle of near-surface temperature, pressure, wind speed, and direction are reasonably captured by the model. However, systematic and interrelated temperature and wind speed biases are present during certain times of day. Uniformly increasing the surface roughness in the model, or implementing a variable surface roughness scheme, may be the most efficient approach toward solving this problem. A negative surface pressure bias exists over the highest elevations of the ice sheet.

In the free atmosphere, the forecasts are of better quality than at the surface, as expected with reduced topographic influence. Radiosonde observations versus the 12–36-h forecasts (over the 2-yr period) at McMurdo Station (coastal site) and Amundsen-Scott South Pole Station (plateau site 2835 m ASL) are examined in order to better understand model performance throughout the atmospheric column. The model performance is qualitatively similar at both stations, despite their different environments. Temperature and geopotential height skill are consistently high throughout the atmospheric column, and biases and NRMS errors are small. Wind speed skill is lowest near the surface; at McMurdo this is due mainly to the zonal component of the wind, which is not as persistent as the topographically influenced meridional component. Wind speed biases are less than ± 1 m s^{-1} at both stations, except near the model top at McMurdo. Dewpoint temperature biases and NRMS errors increase quickly with height.

The impact of the higher-resolution model domains over the McMurdo region is evaluated. It is shown that the 3.3-km domain is more sensitive to spatial and temporal changes in the winds than the 10-km domain, a benefit to forecasters in this region where the weather can change rapidly and topographic influences are dominant. This sensitivity represents an overall improvement in forecast skill, especially on the windward side of the island where the Williams Field and Pegasus runways are situated, and in the lee of Ross Island, an important area of mesoscale cyclogenesis (although the correlation coefficients in these regions are still relatively low).

Overall, the AMPS Polar MM5 produces surprisingly good forecasts considering the complex coastal topography of Antarctica, the limited amount of surface-based observations available for assimilation into the model, and the reduced quality of global analyses in this region. In addition, the system is an ideal example of transferring basic research findings into a product that provides economic, scientific, and human safety benefits. These benefits are evident in that AMPS fa-

cilitates the forecasting decisions that affect the day-to-day activities of the U.S. Antarctic Program. This includes providing important forecast guidance for rescue missions, as well as reducing the number of expensive Antarctic flight "boomerangs" (flights that must turn back to New Zealand because of inclement weather).

Acknowledgments. This research was supported by the National Science Foundation, Office of Polar Programs (UCAR Subcontract SO1-22961) and the National Aeronautics and Space Administration (Grant NAG5-9518). Observations were obtained from the Antarctic Meteorological Research Center at the University of Wisconsin—Madison (Matthew Lazzara), the British Antarctic Survey (Steve Colwell), the Australian Antarctic Data Centre (Neil Adams), and the Space and Naval Warfare Systems Center (Art Cayette). Archived AMPS forecasts were obtained from the NCAR Scientific Computing Division's Data Support Section. Special gratitude is extended to John Cassano for providing code to manipulate MM5 forecast output, and to Sheng-Hung Wang for providing statistical guidance.

APPENDIX

Additional Figures

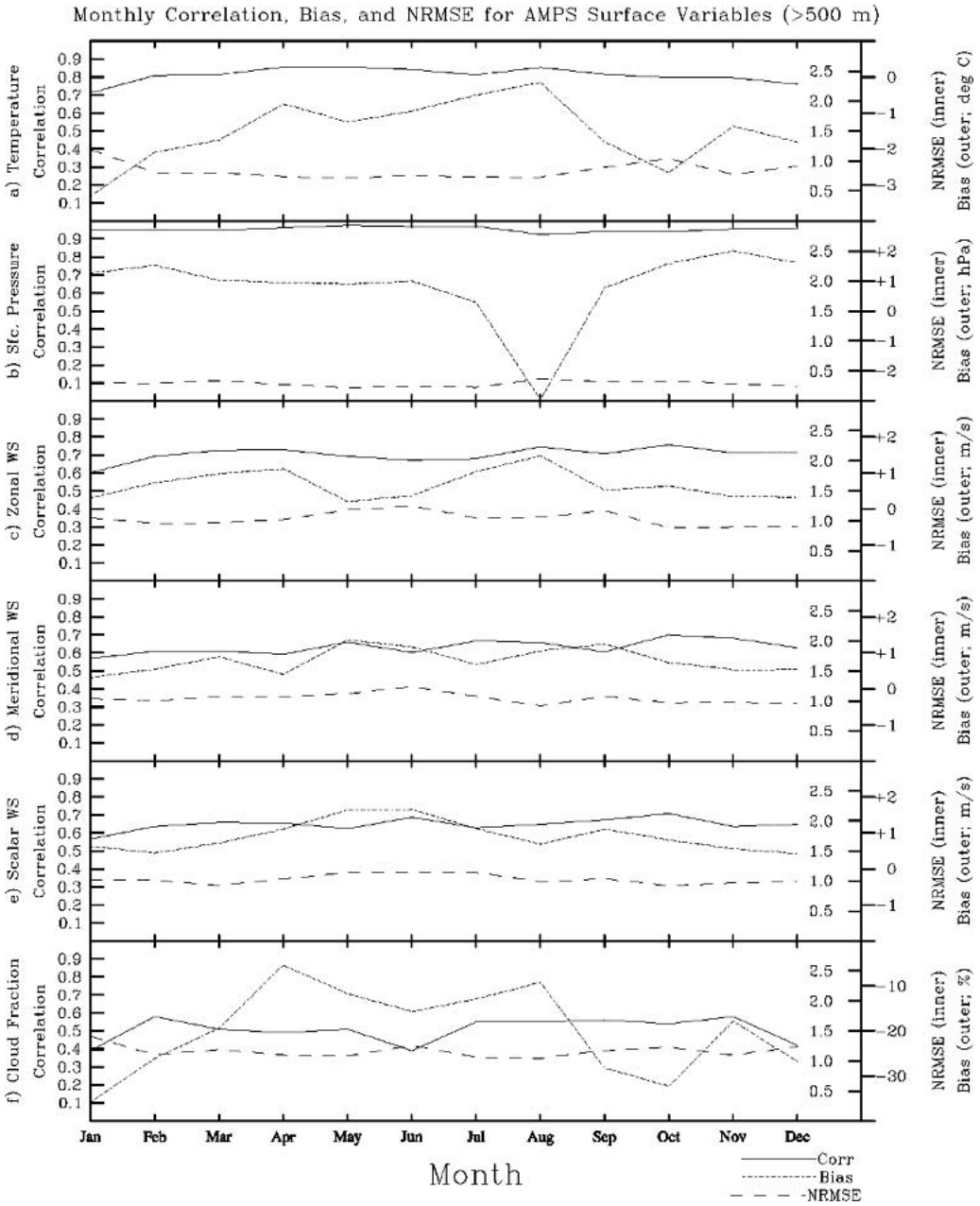

FIG. A1. Same as Fig. 4, but for stations above 500-m elevation. Note that the cloud fraction statistics shown represent only one station above 500 m (South Pole).

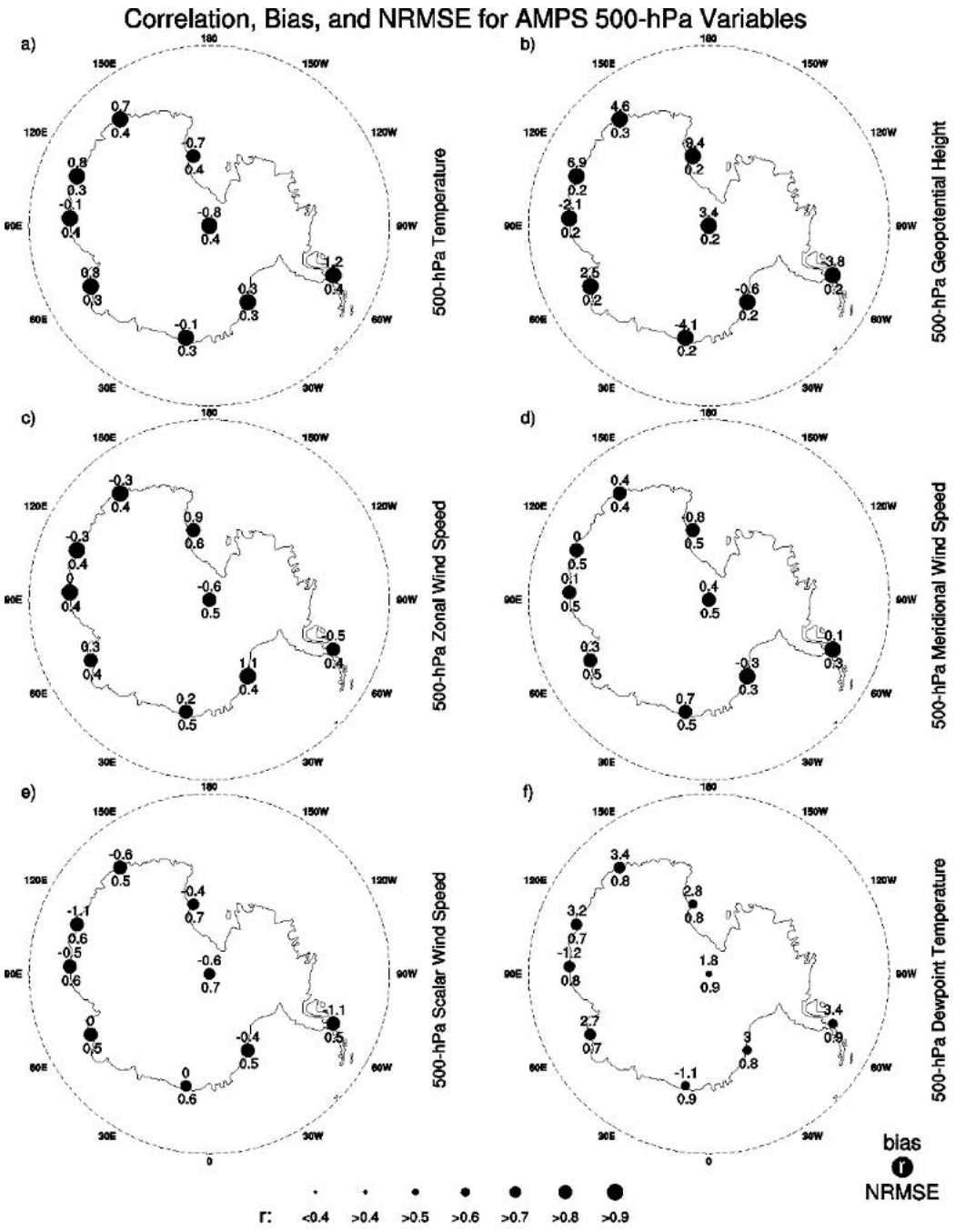

FIG. A2. Similar to Fig. 3, but for 500-hPa (a) temperature, (b) geopotential height, (c) zonal wind speed, (d) meridional wind speed, (e) scalar wind speed, and (f) dewpoint temperature. Bias units are °C, m, and m s^{-1} for temperature (and dewpoint temperature), geopotential height, and winds, respectively.

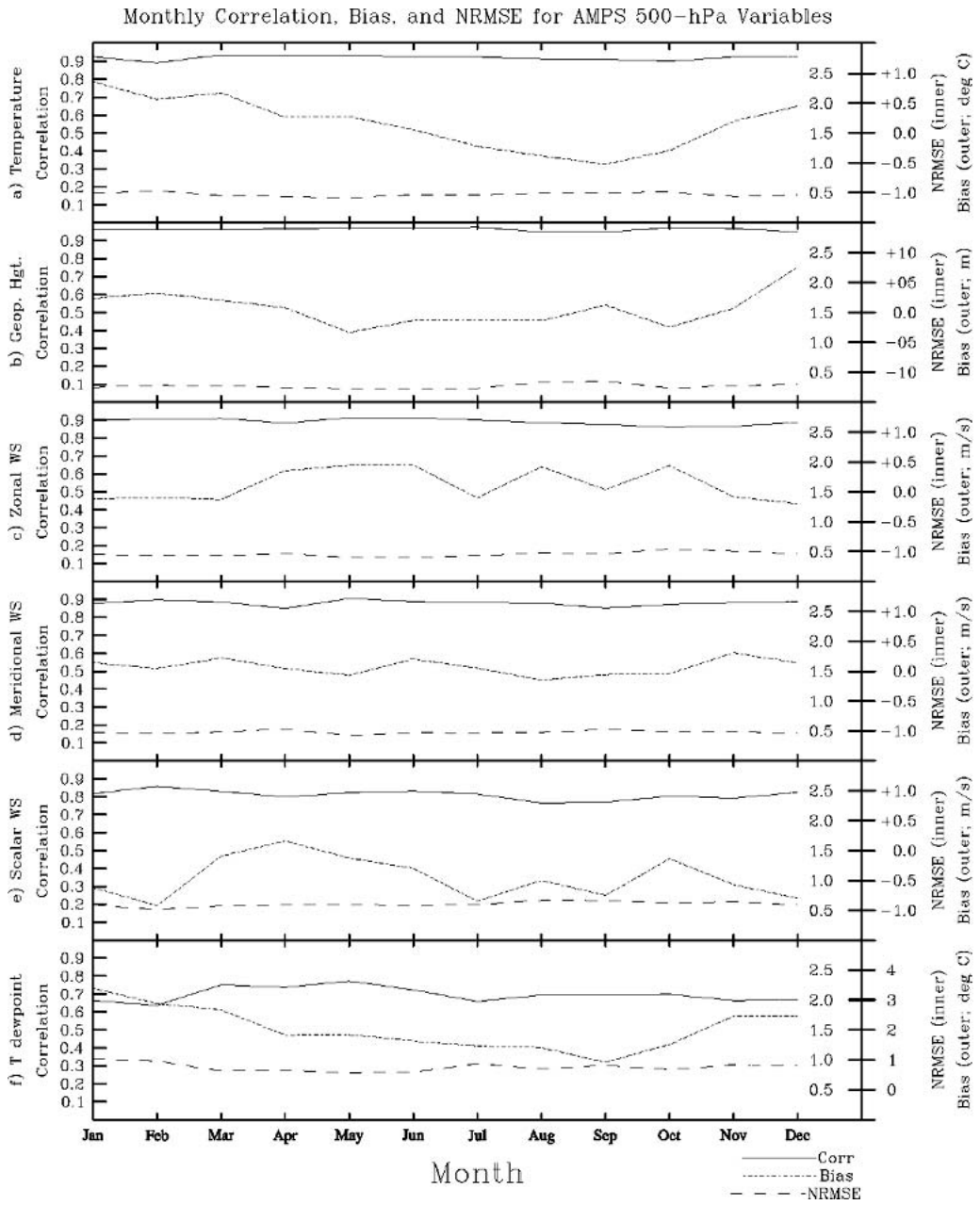

FIG. A3. Similar to Fig. 4, but for 500-hPa (a) temperature, (b) geopotential height, (c) zonal wind speed, (d) meridional wind speed, (e) scalar wind speed, and (f) dewpoint temperature.

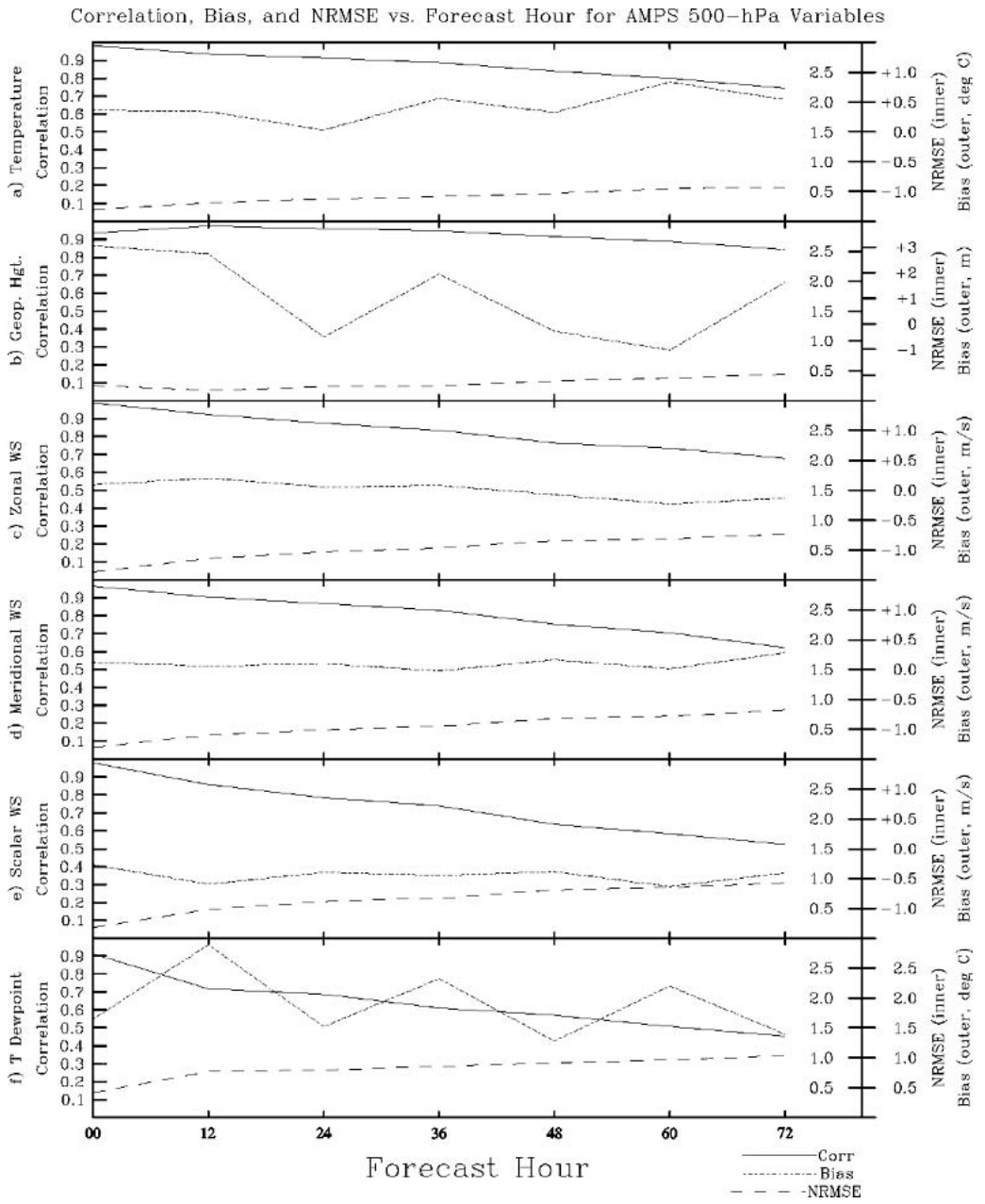

FIG. A4. Similar to Fig. 5, but for 500-hPa (a) temperature, (b) geopotential height, (c) zonal wind speed, (d) meridional wind speed, (e) scalar wind speed, and (f) dewpoint temperature.

REFERENCES

Adams, N., 2004: A numerical modeling study of the weather in East Antarctica and the surrounding Southern Ocean. *Wea. Forecasting,* **19,** 653–672.

Bintanja, R., 2000: Mesoscale meteorological conditions in Dronning Maud Land, Antarctica, during summer: A qualitative analysis of forcing mechanisms. *J. Appl. Meteor.,* **39,** 2348–2370.

——, and M. R. van den Broeke, 1995: Momentum and scalar transfer coefficients over aerodynamically smooth Antarctic surfaces. *Bound.-Layer Meteor.,* **74,** 89–111.

Bromwich, D. H., and J. J. Cassano, 2001: Meeting summary: Antarctic Weather Forecasting Workshop. *Bull. Amer. Meteor. Soc.,* **82,** 1409–1413.

——, ——, T. Klein, G. Heinemann, K. M. Hines, K. Steffen, and J. E. Box, 2001: Mesoscale modeling of katabatic winds over Greenland with the Polar MM5. *Mon. Wea. Rev.,* **129,** 2290–2309.

——, A. J. Monaghan, J. G. Powers, J. J. Cassano, H. Wei, Y. Kuo, and A. Pellegrini, 2003: Antarctic Mesoscale Prediction System (AMPS): A case study from the 2000–01 field season. *Mon. Wea. Rev.,* **131,** 412–434.

——, ——, and Z. Guo, 2004: Modeling the ENSO modulation of

Antarctic climate in the late 1990s with Polar MM5. *J. Climate,* **17,** 109–132.
Budd, W. F., W. R. J. Dingle, and U. Radok, 1964: *Studies in Antarctic Meteorology*. Vol. 9, Antarctic Research Series, Amer. Geophys. Union, 231 pp.
Carrasco, J. F., D. H. Bromwich, and A. J. Monaghan, 2003: Distribution and characteristics of mesoscale cyclones in the Antarctic: Ross Sea eastward to the Weddell Sea. *Mon. Wea. Rev.,* **131,** 289–301.
Cassano, J. J., J. E. Box, D. H. Bromwich, L. Li, and K. Steffen, 2001: Verification of Polar MM5 simulations of Greenland's atmospheric circulation. *J. Geophys. Res.,* **106,** 13 867–13 890.
Cooper, W. A., 1986: Ice initiation in natural clouds. *Precipitation Enhancement—A Scientific Challenge, Meteor. Monogr.*, No. 43, Amer. Meteor. Soc., 29–32.
Davis, J. C., Ed., 1986: *Statistics and Data Analysis in Geology*. 2d ed. Wiley, 646 pp.
Gallée, H., 1998: Simulation of blowing snow over the Antarctic ice sheet. *Ann. Glaciol.,* **26,** 203–206.
Grell, G. L., J. Dudhia, and D. R. Stauffer, 1995: A description of the fifth-generation Penn State/NCAR Mesoscale Model (MM5). NCAR Tech. Note NCAR/TN-398+STR, 117 pp.
Guo, Z., D. H. Bromwich, and J. J. Cassano, 2003: Evaluation of Polar MM5 simulations of Antarctic atmospheric circulation. *Mon. Wea. Rev.,* **131,** 384–411.
Hack, J. J., B. A. Boville, B. P. Briegleb, J. T. Kiehl, P. J. Racsh, and D. L. Williamson, 1993: Description of the NCAR Community Climate Model (CCM2). NCAR Tech. Note NCAR/TN-382+STR, 108 pp.
Hudson, S. R., M. S. Town, V. P. Walden, and S. G. Warren, 2003: Radiosonde temperature, humidity, and pressure response at low temperatures. Preprints, *Seventh Conf. on Polar Meteorology and Oceanography and Joint Symp., on High-Latitude Climate Variations*, Hyannis, MA, Amer. Meteor. Soc., CD-ROM, 4.1.
Janjić, Z. I., 1994: The step-mountain eta coordinate model: Further developments of the convection, viscous sublayer, and turbulence closure schemes. *Mon. Wea. Rev.,* **122,** 927–945.
Kodama, Y., G. Wendler, and N. Ishikawa, 1989: The diurnal variation of the boundary layer in summer in Adélie Land, eastern Antarctica. *J. Appl. Meteor.,* **28,** 16–24.
Liu, H., K. C. Jezek, and B. Li, 1999: Development of an Antarctic digital elevation model by integrating cartographic and remotely sensed data: A geographic information system based approach. *J. Geophys. Res.,* **104,** 23 199–23 213.
Manning, K. W., and J. G. Powers, 2002: Recent modeling issues in AMPS operations. Preprints, *The Antarctic Numerical Weather Prediction and Forecasting Workshop*, Boulder, CO, National Center for Atmospheric Research, 15–17.
Meyers, M. P., P. J. DeMott, and W. R. Cotton, 1992: New primary ice-nucleation parameterizations in an explicit cloud model. *J. Appl. Meteor.,* **31,** 708–721.
Monaghan, A. J., D. H. Bromwich, H. Wei, A. M. Cayette, J. G. Powers, Y. H. Kuo, and M. Lazzara, 2003: Performance of weather forecast models in the rescue of Dr. Ronald Shemenski from South Pole in April 2001. *Wea. Forecasting,* **18,** 142–160.
Nielsen, J. A., 2001: *Icebound: A Doctor's Incredible Battle for Survival at the South Pole*. Miramax, 362 pp.
Nuss, W. A., and D. W. Titley, 1994: Use of multiquadric interpolation for meteorological objective analysis. *Mon. Wea. Rev.,* **122,** 1611–1631.
O'Connor, W. P., and D. H. Bromwich, 1988: Surface airflow around Windless Bight, Ross Island, Antarctica. *Quart. J. Roy. Meteor. Soc,* **114,** 917–938.
Parish, T. R., and D. H. Bromwich, 1997: On the forcing of seasonal changes in surface pressure over Antarctica. *J. Geophys. Res.,* **102,** 13 785–13 792.
——, and J. J. Cassano, 2003: The role of katabatic winds on the Antarctic surface wind regime. *Mon. Wea. Rev.,* **131,** 317–333.
Pendlebury, S. F., N. D. Adams, T. L. Hart, and J. Turner, 2003: Numerical weather prediction model performance over the high southern latitudes. *Mon. Wea. Rev.,* **131,** 335–353.
Periad, C., and P. Pettré, 1993: Some aspects of the climatology of Dumont d'Urville, Adelie Land, Antarctica. *Int. J. Climatol.,* **13,** 313–327.
Powers, J. G., A. J. Monaghan, A. M. Cayette, D. H. Bromwich, Y.-H. Kuo, and K. W. Manning, 2003: Real-time mesoscale modeling over Antarctica: The Antarctic Mesoscale Prediction System (AMPS). *Bull. Amer. Meteor. Soc.,* **84,** 1533–1545.
Puri, K., G. S. Dietachmayer, G. A. Mills, N. E. Davidson, R. A. Bowen, and L. W. Logan, 1998: The new BMRC Limited Area Prediction System, LAPS. *Aust. Meteor. Mag.,* **47,** 203–223.
Renfrew, I. A., 2004: The dynamics of idealised katabatic flow over a moderate slope and ice shelf. *Quart. J. Roy. Meteor. Soc.,* **130,** 1023–1045.
Seefeldt, M. W., G. J. Tripoli, and C. R. Stearns, 2003: A high-resolution numerical simulation of the wind flow in the Ross Island region, Antarctica. *Mon. Wea. Rev.,* **131,** 435–458.
Stull, R. B., 1988: *An Introduction to Boundary Layer Meteorology.* Kluwer Academic, 666 pp.
van Lipzig, N. P. M., E. van Meijgaard, and J. Oerlemans, 2002: The spatial and temporal variability of the surface mass balance in Antarctica: Results from a regional atmospheric climate model. *Int. J. Climatol.,* **22,** 1197–1217.
Weller, G., 1968: The heat budget and heat transfer processes in Antarctic Plateau ice and sea ice. Australian Antarctic Research Expedition (ANARE) Scientific Rep. 4A, No. 102, Australian National Research Expedition, Melbourne, Australia, 155 pp.
Wendler, G., J. C. Andre, P. Pettre, J. Gosink, and T. R. Parish, 1993: *Antarctic Meteorology and Climatology: Studies Based on Automatic Weather Stations.* Vol. 61, *Katabatic Winds in Adelie Coast*. Antarctic Research Series, Amer. Geophys. Union, 207 pp.
——, C. R. Stearns, G. Weidner, G. Dargaud, and T. R. Parish, 1997: On the extraordinary katabatic winds of Adélie Land. *J. Geophys. Res.,* **102,** 4463–4474.